

# JGR Earth Surface

## RESEARCH ARTICLE

10.1029/2019JF005226

### Key Points:

- We used a million measurements to test theory relating bed-sand grain size, suspended-sand grain size, and suspended-sand concentration
- Theory explained most of the range in concentration at constant discharge but less than half of the variability in concentration
- Variability in concentration is also likely due to changes in spatial variability in stress or other properties that are rarely measured

### Supporting Information:

- Supporting Information S1
- Movie S1
- Movie S2
- Movie S3

### Correspondence to:

D. M. Rubin,  
drubin@ucsc.edu

### Citation:

Rubin, D. M., Buscombe, D., Wright, S. A., Topping, D. J., Grams, P. E., Schmidt, J. C., et al. (2020). Causes of variability in suspended-sand concentration evaluated using measurements in the Colorado River in Grand Canyon. *Journal of Geophysical Research: Earth Surface*, 125, e2019JF005226. <https://doi.org/10.1029/2019JF005226>

Received 26 JUN 2019

Accepted 24 JUL 2020

Accepted article online 29 JUL 2020

## Causes of Variability in Suspended-Sand Concentration Evaluated Using Measurements in the Colorado River in Grand Canyon

**D. M. Rubin**<sup>1,2</sup> , **D. Buscombe**<sup>3,4</sup> , **S. A. Wright**<sup>5</sup> , **D. J. Topping**<sup>6</sup> , **P. E. Grams**<sup>6</sup> , **J. C. Schmidt**<sup>7</sup> , **J. E. Hazel Jr.**<sup>3</sup> , **M. A. Kaplinski**<sup>3</sup> , and **R. Tusso**<sup>6</sup> 

<sup>1</sup>Department of Earth and Planetary Sciences, University of California, Santa Cruz, CA, USA, <sup>2</sup>U.S. Geological Survey (Emeritus), Santa Cruz, CA, USA, <sup>3</sup>School of Earth and Sustainability, Northern Arizona University, Flagstaff, AZ, USA,

<sup>4</sup>Marda Science LLC, Flagstaff, AZ, USA, <sup>5</sup>U.S. Geological Survey, Sacramento, CA, USA, <sup>6</sup>Southwest Biological Science Center, Grand Canyon Monitoring and Research Center, U.S. Geological Survey, Flagstaff, AZ, USA, <sup>7</sup>Department of Watershed Sciences, Utah State University, Logan, UT, USA

**Abstract** Rivers commonly exhibit substantial variability in suspended-sand concentration, even at constant water discharge. Here we derive an approach for evaluating how much of this variability arises from mean bed-sand grain size. We apply this approach to the Colorado River in Grand Canyon, where discharge-independent concentration of suspended sand varies by more than a factor of 23 ( $N = 1.4 \times 10^6$ ). Theory predicts that where concentration is controlled by bed-sand grain size, concentration and grain size in suspension will be inversely correlated (i.e., coarsening of the bed causes suspended sand to become coarser in grain size and lower in concentration). Although the observed correlation is negative, riverbed grain size accounts for only 40% of the variability in concentration. The residuals vary by an order of magnitude; they arise from other processes, such as changes in topography or distribution of sand that cause shear stress to change at constant discharge, changes in the fine tail of bed-sand grain sizes or changing bedforms. Both bed sand and the other factors influence concentration for durations from less than 1 day to several years. Predictions of concentration based on bed-sand grain size ( $N = 4 \times 10^4$ ) are less accurate than predictions based on suspended-sand grain size, probably because suspended sand is a natural integrator of sand-transporting processes, giving more weight to those areas of the bed that exchange more sand with the flow. Although the causes of variability vary from one river to another, the approach illustrated here is applicable to any river in which concentration varies at constant water discharge.

## 1. Introduction

### 1.1. Purpose

If all conditions in a river remain constant, then the concentration of suspended sand is expected to remain constant. In many rivers, however, concentration varies at constant water discharge (Colby, 1956; Walling, 1977), thereby demonstrating that conditions other than water discharge change. Annual or flood-event hysteresis is a well-known example of variability in which concentrations at a given discharge differ between the rising and falling limbs of a hydrograph, but variability can also occur without hysteresis (including times when flow is steady), and variability can occur on time scales as long as decades (Horowitz, 2003).

Variability in concentration at a constant discharge has been attributed to many causes including scour and fill (Colby, 1956), changes in amount of sediment stored in a reach (Horowitz, 2003), sediment supply (Moog & Whiting, 1998), changes in grain size of sand on the bed (Rubin et al., 1998; Rubin & Topping, 2001; Topping et al., 2005), changes in water temperature (Colby, 1956), random fluctuations or an “actual change in the relationship” (Colby, 1956), seasonal variability (Colby, 1956; Walling, 1977), evolution or migration of bedforms on the riverbed (Wren et al., 2000), a change in spatial structure of suspended sand in a cross section (Topping & Wright, 2016), turbulence (Wren et al., 2000), and measurement error (Topping et al., 2011). Here we use measurements from the Colorado River in Grand Canyon to quantify the causes of discharge-independent variability in suspended-sand concentration. Specifically, we ask the following:

1. How much of the observed 2–3 orders of magnitude variability in concentration and grain size of suspended sand at a given discharge is explainable by changes in mean grain size of sand on the bed?

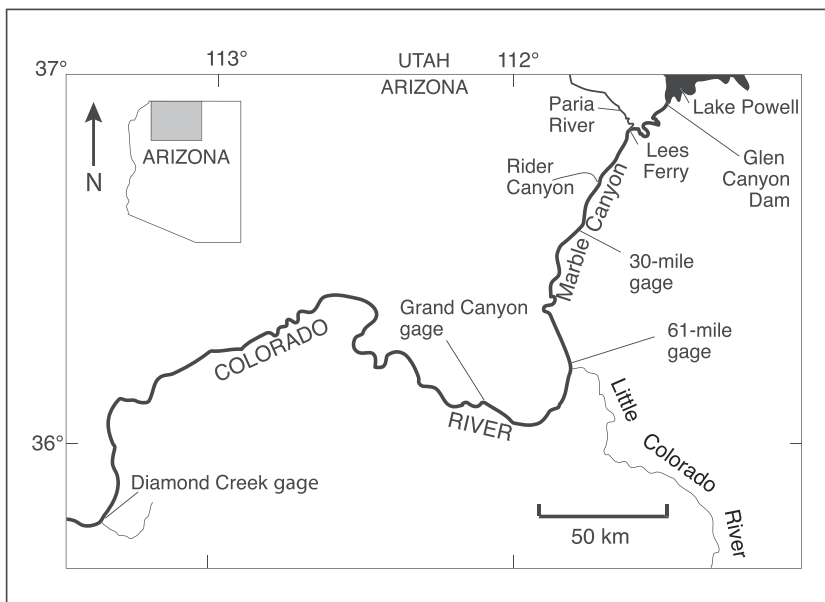


**Figure 1.** Location map showing the Colorado River in Grand Canyon. Suspended-sediment measurements were made at four gages: 30-mile (“USGS 09383050 Colorado River Near River Mile 30”), 61-mile (“USGS 09383100 Colorado R Abv Little rColorado River Near Desert View”), Grand Canyon (“USGS 09402500 Colorado River Near Grand Canyon”), and Diamond Creek (“USGS 09404200 Colorado Rvr Abv Diamond Creek Nr Peach Springs”) (the term “mile” is part of official gage names).

2. Do concentration and grain size of suspended sand covary as predicted by theory (Rubin & Topping, 2001, 2008) for situations where both concentration and grain size in suspension are controlled by bed-sand grain size?
3. Do the temporal and spatial scales of variability constrain the processes that cause variability?

Section 1.5 poses these questions in terms of specific sediment-transport equations that are derived in section 1.4.

Measurements from Colorado River in Grand Canyon are useful for addressing these questions for several reasons. First, a large number of measurements were collected (1.4 million measurements of the concentration and grain size of suspended sand and more than 40 thousand measurements of grain size of sand on the riverbed). Second, the measurements of suspended sand were collected at high frequency (four measurements per hour) and for long duration (more than a decade). This set of measurements is exceptional. Third, the river exhibits substantial variation in concentration (2–3 orders of magnitude) for a constant water discharge, which provides a strong signal to evaluate.

The Colorado River in Grand Canyon is a supply-limited bedrock river (Topping, Rubin, & Vierra, 2000, Topping, Rubin, Nelson, et al., 2000). Although the relative importance of the different causes of variability may differ in other rivers, most of the processes described here also operate in alluvial rivers. The approach used here to evaluate these different causes of variability can be applied to any river in which concentration varies at constant discharge, regardless of geomorphic setting or sediment supply.

## 1.2. Background of Data Collection

Glen Canyon Dam was completed in 1963, 25 km upstream from Lees Ferry (Figure 1), creating the second largest reservoir in the United States. Lake Powell traps all sand, silt, and clay from the 290,000 km<sup>2</sup> upper Colorado River watershed, and the reservoir releases clear, sediment-free water. By the early 1970s, river runners and the National Park Service noticed that sandbars in Marble and Grand Canyons were eroding (Dolan et al., 1974). Today, the remaining sandbars that are emergent at baseflows are extensively used as campsites by more than 20,000 recreational boaters who travel through Grand Canyon each year.

To support efforts to maintain and/or increase the area of sandbars, Glen Canyon Dam releases controlled floods after the Paria River delivers sufficient amounts of sand to the Colorado River. The goal of these

controlled floods is to redistribute the tributary-sand inputs from the channel bed to lateral separation eddies adjacent to the main flow and downstream from most rapids. The Bureau of Reclamation uses sand-transport models to identify the magnitude and duration of a controlled flood that will transport most of, but not more than, that year's sand input (Grams et al., 2015; Wright et al., 2010). This program requires nearly continuous sand-transport measurements, and this paper is based on those measurements.

### 1.3. Hydrologic and Geomorphic Setting

Streamflow of the Colorado River in Grand Canyon is entirely regulated by Glen Canyon Dam, but the sand supplied to this segment of the Colorado River is temporally and spatially decoupled from the flow regime. Between 1990 and 2019, 92% of the Colorado River's total streamflow came from Lake Powell, and only 8% came from tributaries and springs that enter the river downstream from the dam. In contrast, all of the sand supplied to the Colorado River comes from the downstream tributaries, primarily in late summer and fall during the season of the North American monsoon. The months of largest total reservoir releases are in winter and summer when regional electricity demand is greatest.

Although tributaries deliver more silt and clay than sand, sand is the focus of modern sediment management. During periods of tributary flash flooding, most of the silt and clay are quickly transported to Lake Mead reservoir at the downstream end of Grand Canyon. In contrast, most of the sand supplied from tributaries temporarily accumulates on the bed of the Colorado River.

Between 1 July 2004 and 30 June 2019, an average of  $1.7 \times 10^6$  metric tons/year of sand was transported by the Colorado River past the most downstream gage, located 25 km upstream from Lake Mead (USGS Gage 09404200, Colorado River above Diamond Creek). The majority of the sand came from the Paria River ( $0.91 \times 10^6$  metric tons/year). The Little Colorado River delivered  $0.67 \times 10^6$  metric tons/year of sand during the same period, but the Little Colorado enters the Colorado River 100 km downstream from the Paria and is not available for rebuilding sandbars in Marble Canyon.

The geomorphology and sedimentology of the rapids, pools, lateral recirculation eddies, and sandbars have been extensively described and reviewed (Schmidt & Grams, 2011). Grand Canyon has hundreds of rapids. Nearly all of these rapids are formed by debris flows that deliver large boulders to the Colorado River. These boulders cannot be transported by the mainstem flow, and they anchor the fundamental geomorphic organization of the river: the fan/eddy complex (Schmidt & Rubin, 1995). Flow is ponded upstream from each rapid, and lateral separation eddies occur downstream from each rapid. Some sand is advected into the eddies, and the rest is transported downstream.

Despite the fact that the Colorado River in Grand Canyon is known for its rapids, boulders, and bedrock, a substantial proportion of the bed is sandy. Grams et al. (2018) mapped a 50-km segment and estimated that 85% of the bed in eddies and approximately 60% of the bed elsewhere was covered by sand in 2012. Episodic inputs of sand, silt, and clay from tributary flash floods cause temporary fining of bed grain size, which clear-water dam releases scour and winnow, typically within a few months or years (Grams et al., 2015, 2018; Topping, Rubin, Nelson, et al., 2000).

Insight into the varying concentrations of suspended sand during steady releases came from measurements made during the 1996 controlled flood when reservoir releases were  $1,290 \text{ m}^3/\text{s}$  for 7 days. During the week of steady flow, median bed-sand grain size at several locations increased approximately 30%, which caused the concentration of suspended sand to decrease by approximately 50% and caused the grain size of sand in suspension to increase 50% (Rubin et al., 1998; Topping et al., 1999). This was the first evidence of how rapidly grain size on the bed could change, and how those changes could control suspended-sand concentration in Grand Canyon. Topping, Rubin, and Vierra (2000) subsequently showed that sand-supply limitation was evident even in the predam river. Winnowing of sand on the bed during floods produced inversely graded flood deposits, both before and after the river was dammed (Draut & Rubin, 2013; Rubin et al., 1998; Topping, Rubin, Nelson, et al., 2000; Topping et al., 2005, 2006).

### 1.4. Theoretical Background

The suspended-sediment theory underlying this work was developed by Rouse (1937, 1938, 1939), but that theory is impractical to apply in the field, particularly to large rivers with complicated topography that causes shear stress to vary spatially. Rubin and Topping (2001, 2008) used McLean's (1992)

implementation of Rouse's theory to model concentration and grain size of suspended sand for thousands of flow and bed-sand conditions. They then approximated the model results with simpler equations that use measurements that are commonly made in rivers. The simpler equations have the form of sand-transport power laws of Engelund and Hansen (1967). Rubin and Topping (2001, 2008) evaluated the exponents in those power laws by best fit solutions to the thousands of model results.

The Rouse theory demonstrates that for steady, uniform flow in a turbulent boundary layer, the vertical concentration gradient depends on two competing processes: downward settling of grains due to gravity and upward transport of grains due to turbulent diffusion. Rouse derived an expression for the concentration profile, whereby the vertical gradient depends on the ratio of settling velocity to shear velocity (Vanoni, 1975). Because settling velocity depends on grain size, and shear velocity depends on flow strength, the Rouse formulation is an expression of the balance between grain-size effects and flow effects.

In order to apply Rouse's equations, the concentration at the bed must be specified as a boundary condition. This is difficult because concentrations near the bed can approach 50–60% by volume and, moreover, concentration varies substantially with very small differences in distance from the bed. Consequently, concentration is specified at some arbitrarily small distance above the bed, with different researchers selecting different elevations (Camenen & Larson, 2008; Garcia & Parker, 1991; Smith & McLean, 1977; van Rijn, 1984).

Using Rouse's equations, a near-bed concentration predictor, and an assumed velocity profile (e.g., log law), suspended-sediment flux can be calculated by integrating over depth for known shear velocity and bed grain size. This procedure has been the basis of most suspended-sediment load predictors since its introduction by Einstein (1950). Since then, many improvements have been proposed and implemented, such as accounting for high-concentration conditions (Einstein & Chien, 1953), incorporating the effects of density stratification (McLean, 1992; Smith & McLean, 1977; Wright & Parker, 2004a, 2004b), treating particle-particle interactions and inertia (Greimann & Holly, 2001), considering of the effects of sediment-starved bed conditions (Grams & Wilcock, 2007; Topping et al., 2007), considering wave-generated flows (Camenen & Larson, 2008), and accounting for mixed grain sizes and nonequilibrium conditions (Dorrell et al., 2013). Despite these improvements, the fundamental balance between settling and turbulent diffusion identified by Rouse remains the theoretical framework used to interpret and compute suspended-sediment transport rates. Garcia (2008) provides a more thorough review.

Rouse's formulation has been tested and confirmed extensively in laboratory experiments, but it is difficult to test and apply in the field. In the lab, flows can be made steady and uniform, and bed grain size can be kept constant. Application of Rouse's formulation to a natural river, however, requires measurements that are extremely difficult and time-consuming to make. Reach-averaged shear stress and reach-averaged bed-sand grain size are insufficient for Rouse's formulation because bed shear stress and bed grain size can be highly variable in space, due to channel complexity (rapids, riffles, pools, bars, meanders, dunes, sand patches). Application of Rouse's approach would require detailed maps of both shear-stress and bed grain size, which could then be used to make at-a-point calculations of suspended sand based on the local conditions. Such data are rare, if ever, available for a large river.

To avoid the limitations described above, Rubin and Topping (2001, 2008) developed a simpler approach that can be applied using two measurements that are commonly collected in rivers: velocity-weighted concentration and grain size of suspended sand. Rubin and Topping formulated the problem in terms of two dependent variables (concentration and grain size in suspension) and two independent variables (shear velocity and bed-sand grain size). They calculated the relations between the dependent and independent variables for thousands of conditions using McLean's (1992) Rouse-based model. The effects of dunes and bed-sand grain-size variance were incorporated. The model results were then approximated with power law fits relating the dependent and independent variables, thereby providing a simplified approximation of Rouse's theory.

The equations to which Rubin and Topping (2001, 2008) fit the model results follow Engelund and Hansen (1967), who expressed concentration of suspended sand  $C$  as

$$C \propto u_*^J D_b^K, \quad (1)$$

where  $u_*$  is shear velocity and  $D_b$  is median grain size of sand on the bed. Rubin and Topping evaluated  $J$  and  $K$  by solving for the best fits to the thousands of model results as described above. Those exponents

**Table 1**

*Errors in Acoustical Measurements of Suspended Sand as a Function of Suspended Sand Concentration C*

	C (mg/l)	Relative error in concentration (%)		Relative error in grain size (%)	
		68% confidence	95% confidence	68% confidence	95% confidence
Total “error” from all sources including extrapolation and structure of suspended sand in channel (based on equations embedded in figure 22 of Topping & Wright, 2016)	B6110 <sup>0</sup> 10 <sup>1</sup> 10 <sup>2</sup> 10 <sup>3</sup>	125 70 39 21	247 138 77 43	18	34
Error without extrapolation (estimated from Topping et al., 2011, figure 15 and eq 27), but including errors due to spatial structures in suspended-sand concentration	B6010 <sup>0</sup> 10 <sup>1</sup> 10 <sup>2</sup> 10 <sup>3</sup>	42 23 13 7.3	82 46 26 14	6	11
Estimated measurement error for the median concentration	40	17	32	6	11

were evaluated with model results for narrow and wide standard deviations of bed-sand grain size and presence or absence of dunes. For the four combinations of these two conditions,  $J$  ranged from 3.5 to 5.0, and  $K$  ranged from -3.0 to -1.5. Using the same approach of fitting the exponents to model results, Rubin and Topping (2001, 2008) found that grain size of sand in suspension  $D_s$  varies as

$$D_s \propto u_*^L D_b^M, \quad (2)$$

where  $L$  and  $M$  have values of 0.15 to 0.4 and 0.5 to 1.0, respectively.

To quantify the relation between  $C$  and  $D_s$  (left sides of Equations 1 and 2), Equation 2 can be rearranged to solve for  $D_b$ , and that expression substituted for  $D_b$  in Equation 1

$$C \propto u_*^{J - (KL/M)} D_s^{K/M}. \quad (3)$$

In situations where  $u_*$  is constant, Equation 3 simplifies to

$$C \propto D_s^{K/M}. \quad (4)$$

For the four sets of model results (dunes or no dunes; narrow or wide standard deviation of bed-sand grain sizes),  $K/M$  ranges from -4.3 to -2.5 (Rubin & Topping, 2008, Table 1). Rubin and Topping tested this model-derived equation using flume data (Guy et al., 1966) and found  $K/M$  to vary over a slightly wider range (-4.8 to -1.9) than predicted. Topping et al. (2010) used other methods and found  $K/M$  to equal -3.3 for the Colorado River. Though formulated slightly differently (individual grain size bins instead of median values), the model developed by Wright et al. (2010) for computing sand transport rates in Grand Canyon used a value -3.0 for the exponent relating  $C$  to  $D_s$ .

The negative values of  $K/M$  indicate that for the conditions for which Equation 4 was derived (including constant  $u_*$ ),  $C$  and  $D_s$  are inversely correlated; coarsening of the bed causes coarser sand in suspension because that is what is available on the bed, and coarsening simultaneously causes lower concentrations of suspended sand because the coarser sand is less readily suspended due to higher settling velocity. Equation 4 is particularly amenable to field application because it requires only measurements of two commonly measured variables (concentration and grain size of suspended sand). Observations are not required of the more difficult-to-measure independent variables ( $u_*$  and  $D_b$ ).

Concentration of suspended sand can be related to grain size on the bed  $D_b$  rather than to grain size in suspension  $D_s$  with a few modifications to Equation 1. First, concentration  $C$  and  $D_b$  can be expressed as normalized values by dividing the observed values by their respective temporal means ( $\bar{C}$  and  $\bar{D}_b$ ). Second, restricting the equation to any constant value of  $u_*$  allows that term to be incorporated in the proportionality and eliminated from the equation.

$$\frac{C}{\bar{C}} \propto \left( \frac{D_b}{\bar{D}_b} \right)^K \quad (5)$$

Equation 5 illustrates that for a constant value of  $u_*$ , normalized concentration of suspended sand is proportional to normalized bed-sand grain size raised to a power of  $K$ , which was found to range from  $-3.0$  to  $-1.5$  (Rubin & Topping, 2001).

### 1.5. Research Questions Rephrased in Terms of Equations 4 and 5

The questions addressed in this paper can be rephrased precisely in terms of the equations derived above: Are concentration and grain size of suspended sand related as predicted by Equation 4, with values of exponent  $K/M$  within the predicted range? Is  $K/M$  constant over time and location, or does it vary? How much variability in concentration at constant discharge is accounted for by changes in bed-sand grain size? What physical processes cause variability that is not accounted for by Equation 4? Are there specific times when Equation 4 is more or less accurate than other times? How well does Equation 5 predict suspended-sand concentration when bed-sand grain size changes?

The performance of the equations is evaluated using several statistics: Measurements of  $C$  and  $D_s$  are used to solve for the best fit values of  $K/M$  (Equation 4) and compared to the predicted range. Squared correlations between  $\log C$  and  $\log D_s$  and between  $C$  and  $D_b$  are used to measure the proportion of covariance is accounted for by Equations 4 and 5. Observed deviations from these equations are then used in conjunction with other lines of evidence reported in the literature, to infer what processes the equations do not describe adequately.

## 2. Measurement Methods

### 2.1. Bed-Sand Measurements and Errors

Grain size of sand on the riverbed was measured using digital images instead of physical sampling (Chezar & Rubin, 2004; Rubin, 2004; Tusso et al., 2020). A video camera and light source were enclosed in a 50-kg wrecking ball that was lowered to the bed with an electric winch (Rubin et al., 2007). The wrecking ball protected the video camera and helped it sink to the bed even in strong currents. At each sampling location along a cross section, three to five digital images of sand were taken through a window resting directly on the bed. Because the window rested directly on the sandy bed, image quality was not degraded by turbidity.

Until 2009, bed-sand grain size was measured using a 2-D autocorrelation algorithm that measured the arithmetic mean size of grains in individual digital images (Rubin, 2004; Rubin et al., 2007). These arithmetic means could not be converted to the sedimentologically preferable geometric mean or median for individual images, but geometric means were calculated for sets of these arithmetic mean sizes. Thus, the term “geometric mean” used below refers to the geometric mean size of a set of images, with each individual image measured by its arithmetic mean. Similarly, the geometric standard errors reported below were calculated from the geometric standard deviation of the arithmetic means. Beginning in 2009, higher-resolution images were collected, and a wavelet algorithm was used to calculate a full grain-size distribution (Buscombe, 2013). Arithmetic mean grain size was calculated from this distribution, so as to retain consistency with the earlier results.

Errors arising from both methods—determined by comparison with mechanical sieving, with manual point counts in individual images, and with comparison with mathematically simulated particles—are random rather than biased and are typically on the order of 10% for the mean size (Barnard et al., 2007; Buscombe, 2013; Buscombe & Rubin, 2012; Buscombe et al., 2010; Rubin, 2004; Rubin et al., 2007, Table 4; Warrick et al., 2009; and Supporting Information S1). The work presented here compares spatial and temporal trends of large sample populations rather than individual measurements, and results are typically based on dozens to thousands of observations. Consequently, the standard error of the mean is typically only a few percent, which is 1–2 orders of magnitude less than the observed changes in mean bed-sand grain size.

Digital grain-size analysis offers several advantages over traditional sampling. Digital techniques are rapid and inexpensive in both the field and lab, enabling tens of thousands of grain-size measurements. In addition, most physical samplers unavoidably include subsurface grains, which are not interacting with the flow. In contrast, digital imaging of grains on the bed surface measures only those grains that are interacting directly with the flow.

Locations of the sampling boat (a 7-m-long pontoon raft described by Rubin et al. (2007, Figure 2a) were mapped using several techniques. On the earliest surveys, longitudinal distance was determined by sighting from maps, and cross-channel location was determined by visual estimates. On later surveys, locations were determined from established survey control points with a shore-based laser-tracking system (Hazel et al., 2008) or determined by GPS. Grain size of bed sand was sampled more densely in the 125 km upstream from the Little Colorado River because previous work demonstrated that bed-sand grain size in this part of the river changes more rapidly and with greater magnitude than farther downstream in response to large floods on the Paria River (Topping, Rubin, Nelson, et al., 2000).

Elevation of the water surface was determined from either stage-discharge relations (Hazel et al., 2006) with respect to the elevation of typical base flow ( $227 \text{ m}^3/\text{s}$ ) or modeled water-surface elevations (Magirl et al., 2008). Depths to the riverbed were measured either by markings on the video cable lowered to the riverbed or from multibeam surveys of the river channel (Kaplinski et al., 2017). Each sampling location was characterized as either main channel or lateral separation eddies, based on geomorphic maps (Grams et al., 2018).

When the bed-sampling work was initiated in 2000, the strategy was to collect large numbers of samples on cross-channel transects, excluding regions where the bed was coarser than sand. These early surveys generally covered the same regions in each river segment, but the regions were not necessarily sampled representatively with respect to depth or geomorphic setting. We used several approaches to address potential bias arising from nonrepresentative sampling in the early surveys. To eliminate effects of nonrepresentative sampling by depth, the data were grouped in individual depth bins. To eliminate effects of nonrepresentative sampling by geomorphic setting, the differences between sand in the main channel and in eddies were evaluated, and the relatively small difference suggests that bias of possible nonrepresentative sampling of geomorphic settings is unlikely to introduce a bias of more than 10–20%. Systematic errors of 20% would require some surveys to be entirely channel sand and others to be entirely eddy sand; such extreme nonrepresentative sampling never occurred. In 2011, the sampling strategy shifted to an unequally spaced grid design to reduce or eliminate potential nonrepresentative sampling.

## 2.2. Suspended-Sand Measurements and Error

Concentration and grain size of sand in suspension were measured every 15 min at the four gages (Figure 1), using the multifrequency acoustical methods of Topping and Wright (2016). These measurements were made using bank-mounted side-looking acoustic-Doppler profilers. These profilers were mounted adjacent or near each other at the 30-mile, Grand Canyon, and Diamond Creek gages, and on opposite banks at the 61-mile gage. Thus, the different-frequency profilers ensonified similar water-sediment mixtures at the first three gages, and potentially different water-sediment mixtures at the 61-mile gage. The beam-averaged attenuation and backscatter at multiple frequencies were used to measure silt-and-clay concentration, sand concentration, and sand median grain size. The instruments together sampled approximately 10% of the channel width and a fraction of a percent of the flow depth for a duration of 4 min. The main use of these measurements was to calculate the total sediment flux for the full cross section, which required that the local acoustical measurements be calibrated with Equal-Width-Increment (EWI) or Equal-Discharge-Increment (EDI) measurements (Edwards & Glysson, 1999; Griffiths et al., 2012).

Although the measurements include the small amount of spatial averaging described above, they are approximately “at-a-point” measurements when compared to standard EWI or EDI measurements. Topping and Wright (2016) discuss how spatial and temporal variability can cause substantial error (both random error and nonrandom time-varying error) in extrapolating from one part of the channel to the full cross section. For the present goal of measuring and understanding changes in suspended sand at a point, measurements are not extrapolated, and, moreover, changes in spatial structure of suspended sediment (e.g., Topping et al., 2011) as well as any other real changes in the channel are considered signal rather than noise or error. Estimates of error in the at-a-point measurements, therefore, must exclude “errors” arising from extrapolation and from variability due to physical processes in the channel.

Errors in the at-a-point measurements (Table 1) were calculated using equations within Figure 22 of Topping and Wright (2016), and the errors calculated using these equations are shown here in the first row in Table 1. According to Topping et al. (2011, Figure 15), extrapolating suspended-sand concentration measured at one up-down vertical profile of suspended sediment to the full channel increases the error in

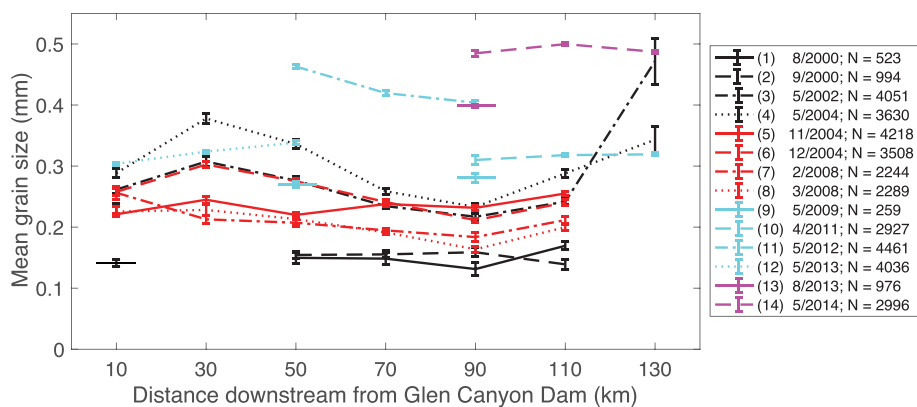


**Figure 2.** Mean grain size of sand on the bed as a function of longitudinal distance for 14 surveys. Grain size varies more among surveys than among river segments. The median ratio of maximum to minimum grain size for all surveys at any location is 2.5, whereas the median ratio of maximum to minimum grain size for all locations at any one time is 1.3. N gives the total number of measurements for each survey. Each plotted value is the geometric mean of the arithmetic mean sizes determined from images. Error bars show the geometric standard error of the mean.

an EWI or EDI measurement by a factor of 3. Thus, we estimate that measurement error alone (second row in Table 1) is 33% of the total error. We assumed the same 33% ratio of measurement error to total error for grain-size measurements.

Errors in concentration do not exceed a few tens of percent, except when measured concentrations are very low, in which case the errors are many tens of percent. Although these errors are substantial, the range of concentrations leading to the conclusions presented below are typically an order of magnitude greater. Errors in  $D_s$  are also an order of magnitude smaller than the observed changes. These errors have a slight grain-size dependent bias.

Several factors suggest the errors are smaller and less likely to lead to false conclusions than the numbers listed in Table 1. First, the errors reported in Table 1 are for individual measurements, whereas the results discussed below are based on correlations between 96 measurements on individual days or based on hundreds to hundreds of thousands of observations spread out over months or years. Random errors in such large populations might degrade correlations but are unlikely to cause spurious correlations. Second, the errors estimated by Topping and Wright (2016) include measurements with high silt and clay concentrations, but our analyses exclude measurements when the silt and clay concentration was greater than 5,000 mg/L or when it was greater than five times the sand concentration. This conservative approach means that the results are more definitive, although our approach may have excluded real patterns during muddy conditions.

### 3. Results

#### 3.1. Bed Sand

Both casual inspection and bed-material surveys (Anima et al., 1998; Schmidt et al., 2007) have shown that different regions of the riverbed consist of boulders, cobbles, or bedrock, as well as areas covered in sand. Despite this great spatial variability, with few exceptions, mean grain size of sand averaged over 20-km-long segments was observed to vary little longitudinally over a 120-km distance during each individual survey (Figure 2). This limited longitudinal variability is not surprising given that none of the surveys were conducted soon after a large Paria River flood (unlike the 1998 case described by Topping, Rubin, Nelson, et al., 2000). In contrast, the average grain size for each survey varied more than threefold between a fine bed condition of ~0.15 mm and a coarse bed condition of ~0.5 mm (Figure 2).

In contrast to the limited longitudinal variability, grain size varied greatly with depth and from one survey to another. Sand in pools deeper than 20 m was coarser than in shallower parts of the river (Figure 3). This trend occurred on some individual surveys, but it is most evident when measurements from all surveys are averaged (Figure 3b). Mean grain size at a depth of -20 to -25 m (referenced to the water-surface elevation at baseflow, 227 m<sup>3</sup>/s) was 0.5 mm, which was more than twice the grain size at the water's edge (0.2 mm). For constant depths, mean grain size of sand on the bed varied among surveys by as much as a

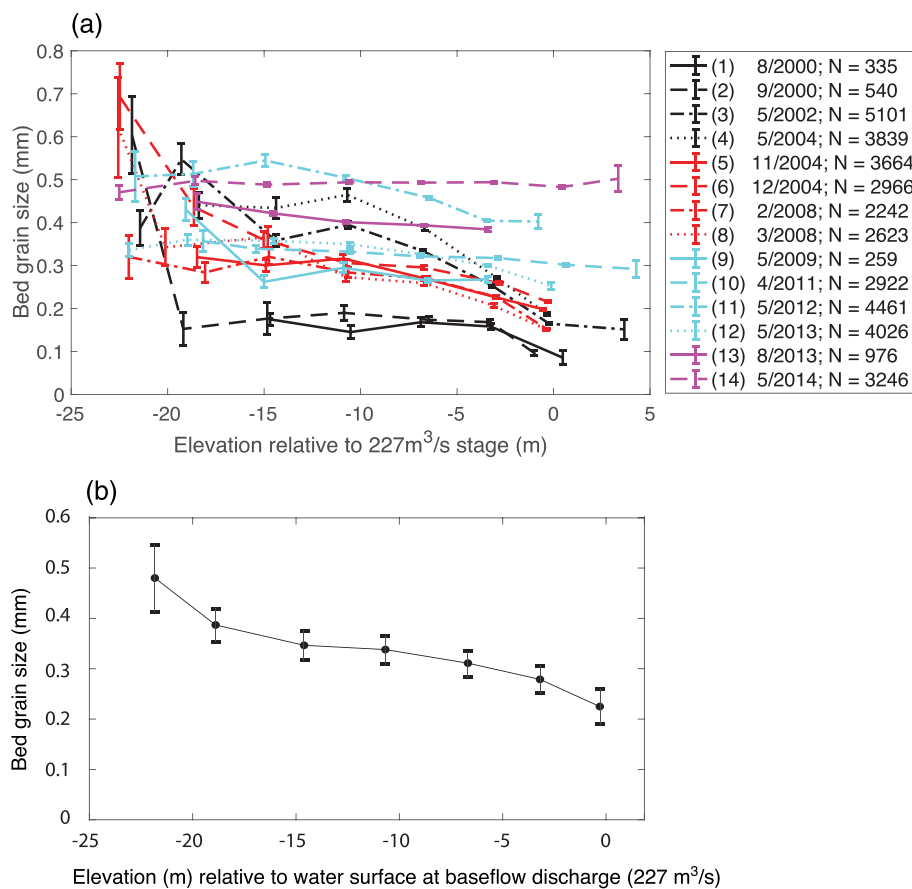


**Figure 3.** Mean grain size of sand on the bed plotted as a function of riverbed depth for all observations at depths of +5 to −25 m between Lees Ferry and the confluence of the Little Colorado River. Grain size of sand on the bed coarsens from the water's edge to the thalweg. Depths are measured relative to river stage of typical baseflow (227 m<sup>3</sup>/s). This discharge had a duration of 80% for instantaneous discharge between 2000 and 2019. (a) Grain sizes observed on individual surveys. Each point shows the geometric mean of the arithmetic means calculated for all grain-size images at the specified depth; error bars indicate geometric standard error. These errors are small except in deep water, where fewer measurements were made. (b) Grain sizes averaged for all surveys. Each point shows the arithmetic mean of the geometric means in (a). Because the observations are clustered in surveys, error bars are calculated using the standard deviation of the points plotted in (a) and the square root of the number of the 14 surveys with observations in each depth bin. Error bars are therefore wider than in (a) because of the smaller number of observations (maximum possible is 14).

factor of 5 (Figure 3a). Bed-sand grain size varied seasonally. The bed was typically coarser when observed in May because the sand transported into the river by tributary flash floods during the previous summer and fall monsoons had undergone many months of winnowing.

The 14 subplots in Figure 4 illustrate how bed-sand grain size varied as a function of three independent variables (survey date, depth to the riverbed, and distance downriver). Of these three variables, the greatest influence on grain size was the date when each survey was conducted. The first survey (August 2000) immediately followed small floods on the Paria River and larger floods on other Marble Canyon tributaries downstream from the Paria River. Those floods delivered fine sand (Schmidt et al., 2007) that covered the bed at all depths and in all river segments that were surveyed (Figure 4). In the spring of 2002 and 2004, the bed was coarser. This coarsening was substantial—particularly in the deepest pools of the channel—with large parts of the river coarsening by a factor of ~4 (Figure 3). The coarsening between 2000 and 2004 occurred during a period when the annual delivery of sand from the Paria River was below average.

On average, the ratio of grain size of sand on the bed of eddies to the bed of the main channel in pools was 0.8. This ratio was determined by comparing grain sizes in the channel and eddies in the 70 km immediately

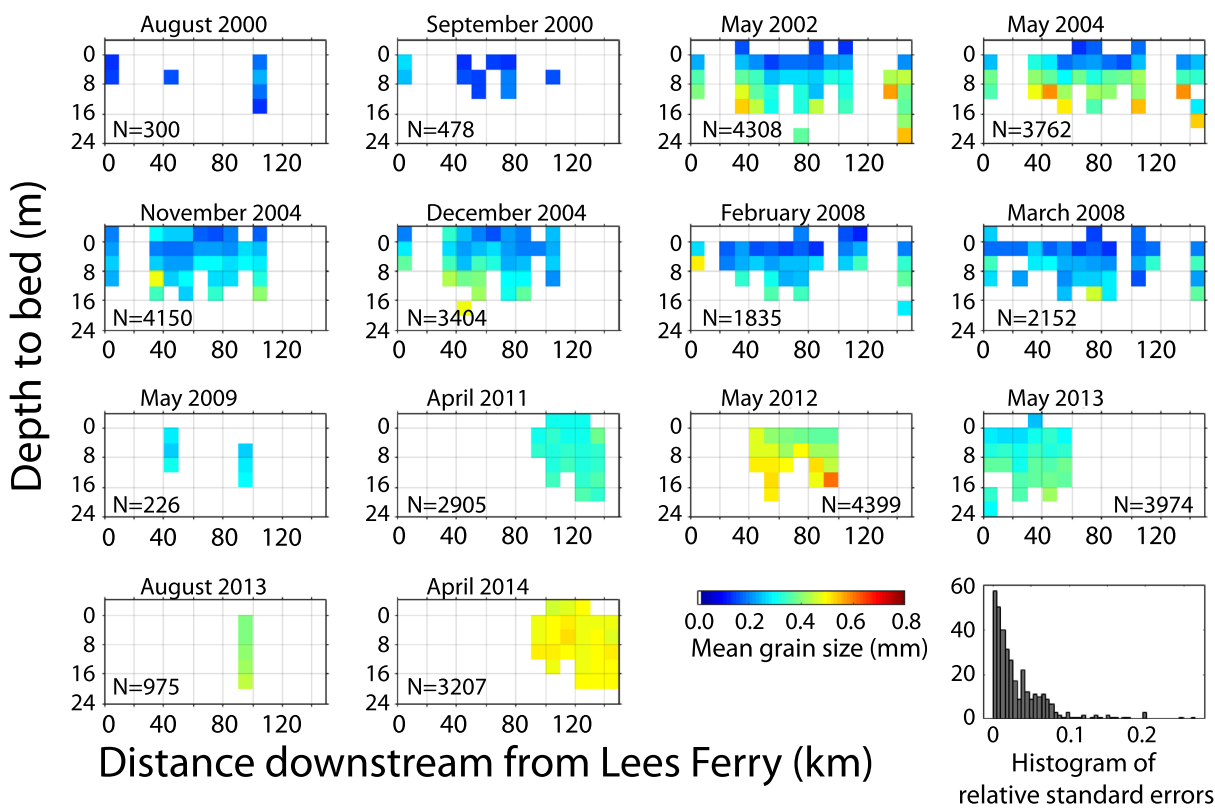


**Figure 4.** Geometric mean grain size of sand on the bed for 14 surveys. Grain size in each bin (10-km distance by 4-m depth) is represented by color (for all bins with at least 12 observations). Sand tends to be coarser where the bed is deeper, and grain size tends to vary more among surveys than among reaches (as also shown in Figures 2 and 3). The first survey (August 2000) was conducted immediately following inputs of fine sand from tributaries, and grain size was fine in all bins sampled. The bed coarsened between then and May 2004, particularly in deeper water. During summer 2004, new inputs from the Paria River caused rapid fining; by December 2004, the bed had coarsened again. The histogram at bottom right shows the number of bins having the specified relative geometric standard error of the mean (standard error of the mean expressed as a percent of the mean). For half of the bins, this error is less than 2.1%, and the maximum error for any bin is 26.4%.

downstream from Lees Ferry using 31 subsets of observations where a survey-measured grain size in both environments in the same distance-depth bin ( $N = 15,337$ ).

### 3.2. Suspended Sand

Measurements of concentration  $C$  and suspended-sand median grain size  $D_s$  at the 61-mile gage show three key features that are qualitatively consistent with Equations 1, 3, and 4. First, concentrations increase with water discharge (Figure 5), as is typical of suspended-sand rating curves. Second, concentration varies by several orders of magnitude for a given water discharge. Third, for a given water discharge  $C$  varies inversely with  $D_s$ .

Ideally, we would test Equation 3 to see how accurately it predicts concentration from  $u_*$  and  $D_s$ , but this is not possible because we have no direct measurements of  $u_*$  or maps of how it varies spatially. Although it might be tempting to use water discharge or reach-averaged  $u_*$  as an approximation, such an approach is flawed. Reach-averaged  $u_*$  includes very high values in rapids and other locations where the bed is usually devoid of sand, and, consequently, the high boundary shear stress in those areas has little influence on suspended sand  $C$  or  $D_s$ . In these regions of the bed, sand is transported as wash load and has minimal interaction with the bed.  $C$  or  $D_s$  through these high-stress areas is determined by flow and bed conditions in the sandy areas of the channel immediately upstream. Reach-averaged  $u_*$  includes the high-stress areas of the channel and is therefore an inappropriate measure to use in Equation 3.

As an alternative to testing Equation 3, we evaluated how well Equation 4 predicts the relationship between  $\log C$  and  $\log D_s$  at constant discharge. This was done by separating the suspended-sand measurements into 94

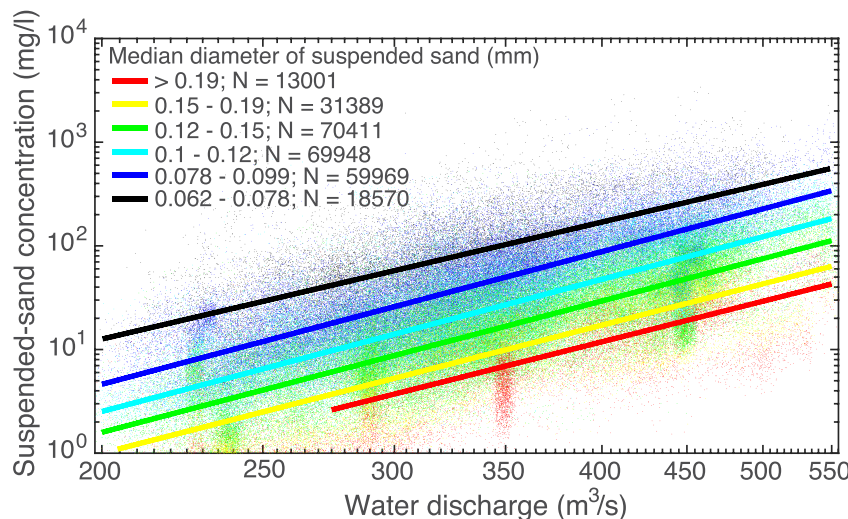


**Figure 5.** Concentration of suspended sand as a function of water discharge at the 61-mile gage. For any given water discharge, the concentration of suspended sand varies by 2–3 orders of magnitude. Each point is color-coded to show grain size of suspended sand; colored lines show the log-space best fit curves for each grain size. Separation into color bands is a visual illustration that concentrations of suspended sand are higher at times when grain size in suspension is finer. Higher concentrations and finer grain size are both consistent with finer sand on the bed.  $R^2$  for regressions fit to individual grain-size fractions range from 0.30 to 0.44.

bins of nearly constant ( $\pm 1\%$ ) discharge between 200 and 1,312 m<sup>3</sup>/s. To eliminate the effects of differing discharge, the log-transformed measurements in each of the 94 subsets were normalized by subtracting from each log  $C$  and each log  $D_s$  measurement the corresponding mean for that discharge bin. As a result of these two transformations (taking the log and normalizing), the mean log  $C$  and mean log  $D_s$  in each subset were zero, and the slope between each measurement and the mean was unaltered (Figure 6a). The best power law solution for the exponent  $K/M$  was then calculated for the several hundred thousand measurements at each gage. These solutions were calculated using reduced major axis regression because  $C$  and  $D_s$  are both dependent variables with error (Davis, 1986, pp. 200–204). The best fit solution of a reduced major axis regression is also symmetrical, meaning the relation does not change when either  $C$  or  $D_s$  is considered the independent variable. The values of  $K/M$  calculated using this procedure are –3.8, –3.6, and –3.1 for the 30-mile, 61-mile, and Diamond Creek gages, respectively.  $K/M$  at the Grand Canyon gage is –5.8, which corresponds to a substantially steeper slope between log  $C$  and log  $D_s$ . Possible causes of this steeper slope are considered in section 4.

The squared correlation ( $R^2$ ) between log  $C$  and log  $D_s$  at the 61-mile gage was 0.45, and the mean  $R^2$  for the four gages was 0.4, indicating that Equation 4 accounted for 40% of the covariance between log  $C$  and log  $D_s$ . Of the 60% that was not accounted for, a small portion was due to measurement error (Table 1), but most of that 60% must arise from sand-transport processes that are not adequately described by Equation 4.

The squared correlation calculated above is one measure of how well Equation 4 describes the relation between log  $C$  and log  $D_s$ , but other statistical measures give additional information. In particular, it is instructive to compare three ranges over which concentration varies at constant discharge: the overall range in  $C$ , the range in  $C$  that is accounted for by Equation 4, and the range of the residuals to Equation 4. At the 61-mile gage (Figure 6a), 95% of the measurements of  $C$  (mean  $C \pm 2$  standard deviations) ranged over a factor of 37. The variability in concentration not accounted for by Equation 4 was approximated by the spread of 95% of the residuals to the best fit power law. At the 61-mile gage, this range was a factor of 14 (illustrated by the dashed lines in Figure 6a). Assuming that the total spread in  $C$  is the sum in quadrature of the spread predicted by Equation 4 and the spread in residuals to Equation 4, the total range of a factor of 37 was decomposed into a factor of 35 that was accounted for by Equation 4 and the factor of 14 spread in residuals. Using the same approach at all four gages gave a mean factor of 23 range in  $C$ , a factor of 20 accounted for by Equation 4, and a factor of 11 range in the residuals. Equation 4 thus accounted for almost twice the range in concentration as other factors. This calculation was somewhat imprecise, however, because the choice of

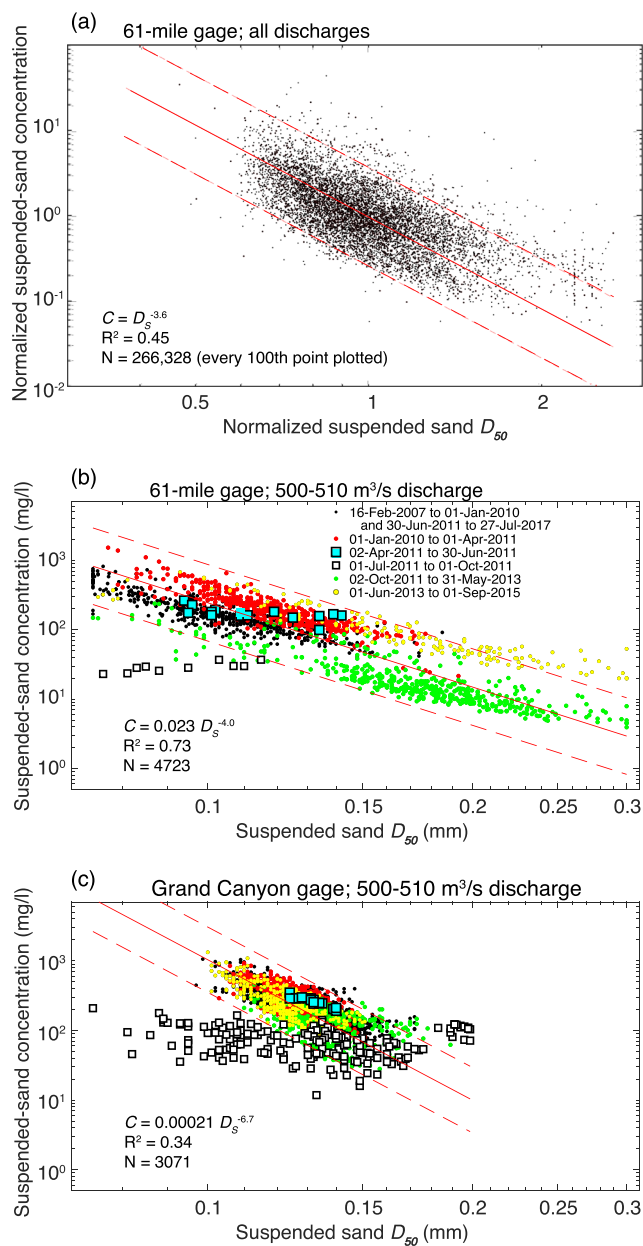


**Figure 6.** Relation between concentration and grain size of sand in suspension. (a) Plot of concentration as a function of grain size of sand in suspension for 94 narrow ( $\pm 1\%$  discharge bins). To test Equation 4, measurements were normalized as described in the text. The solid red line shows the best fit power law; dashed and dotted red lines show ±1 and ±2 standard deviations from the best fit, respectively. Equation 4 predicts that where concentration and grain size in suspension are regulated by grain size on the bed, the slope of the regression line ( $K/M$ ) fit to the log-transformed data should lie between −6 and −3. For this gage, the slope is −3.6. (b) Plot of measurements for a discharge range of 500–510 m<sup>3</sup>/s at the 61-mile gage. Clusters of points from different times are offset from the best fit line for periods as long as several years. These offsets require processes other than changes in mean size of sand on the bed. (c) Measurements for a discharge range of 500–510 m<sup>3</sup>/s at the Grand Canyon gage. Similarities between the fields of points in (a) and (b), from locations 42 km apart, show that the variability had a long spatial scale as well as a long temporal scale.

95% ( $\pm 2$  standard deviations) was arbitrary. Using a larger (or smaller) number of standard deviations to approximate the various ranges attributed a greater (or smaller) proportion of the variability to Equation 4. The first result (that Equation 4 accounted for only 40% of the covariance between  $\log C$  and  $\log D_s$ ) might appear to conflict with the second result (that  $D_s$  accounted for most of the range in  $C$ ), but the two results measure different quantities. The first result is a measure of the proportion of covariance of the logs of the two variables explained by Equation 4; the second result is a measure of approximate total (nonlog) spread explained by Equation 4.

To illustrate how the measurements in Figure 6a vary through time,  $C$  is plotted as a function of  $D_s$  at a single nearly constant discharge (500–510 m<sup>3</sup>/s) in Figure 6b (61-mile gage) and Figure 6c (Grand Canyon gage). In both plots, clusters of points diverge substantially from the best fit power law for periods as long as several years. Some of the subsets in Figures 6b and 6c have different slopes that correspond to different values of  $K/M$ , and other subsets have a similar slope to the best fit solution but are offset to higher or lower  $C$  or  $D_s$ . It is noteworthy that some of the differences between subsets occurred at different gages during the same time periods (Figures 6b and 6c). For example, concentrations in April through June 2011 were lower than concentrations at the same discharge during the following time period (July 2011 through October 2011). The same change occurred at the other two gages (not shown), demonstrating similar behavior at gages spanning a distance of more than 300 km. Moreover, some of these changes also occurred at constant discharges other than the one shown in Figures 6b and 6c.

The preceding results show how  $C$  and  $D_s$  vary independently of discharge over periods of months to years; daily measurements provide information about the processes that influence suspended sand on shorter time periods. The daily patterns are presented as animated sequences in the supporting information, and eight individual days are shown in Figure 7. The eight plots were selected from measurements at two gages to best illustrate a variety of daily patterns in discharge and suspended sand. They were selected from 4,281 daily records in which the silt and clay concentrations do not exceed the limits specified in section 2.

Steady flows only occurred on 14% of the 4,281 days studied, but examining suspended sediment transport on these days is informative because suspended sand is more likely to be in equilibrium with steady flows. The top row of Figure 7 shows three such days at the 61-mile gage when dam releases were steady (in this case defined as less than  $\pm 5\%$  change in discharge). Equations 1 and 2 predict that  $C$  and  $D_s$  will remain constant for constant  $u_*$  and  $D_b$ , but this predicted pattern was relatively rare. It occurred on only 166 of the 599 steady-flow days (Figure 7a shows an example), suggesting that  $u_*$ ,  $D_b$ , or factors that are not addressed by the equations varied on a time scale of hours on most days when flows were steady.

Equation 4 predicts that  $C$  and  $D_s$  vary inversely where  $u_*$  is constant but  $D_s$  changes. This pattern was observed on 474 of the 599 steady-flow days (Figure 7b shows an example). Of the 125 days that did not conform to Equation 4, nearly all occurred at the 61-mile gage

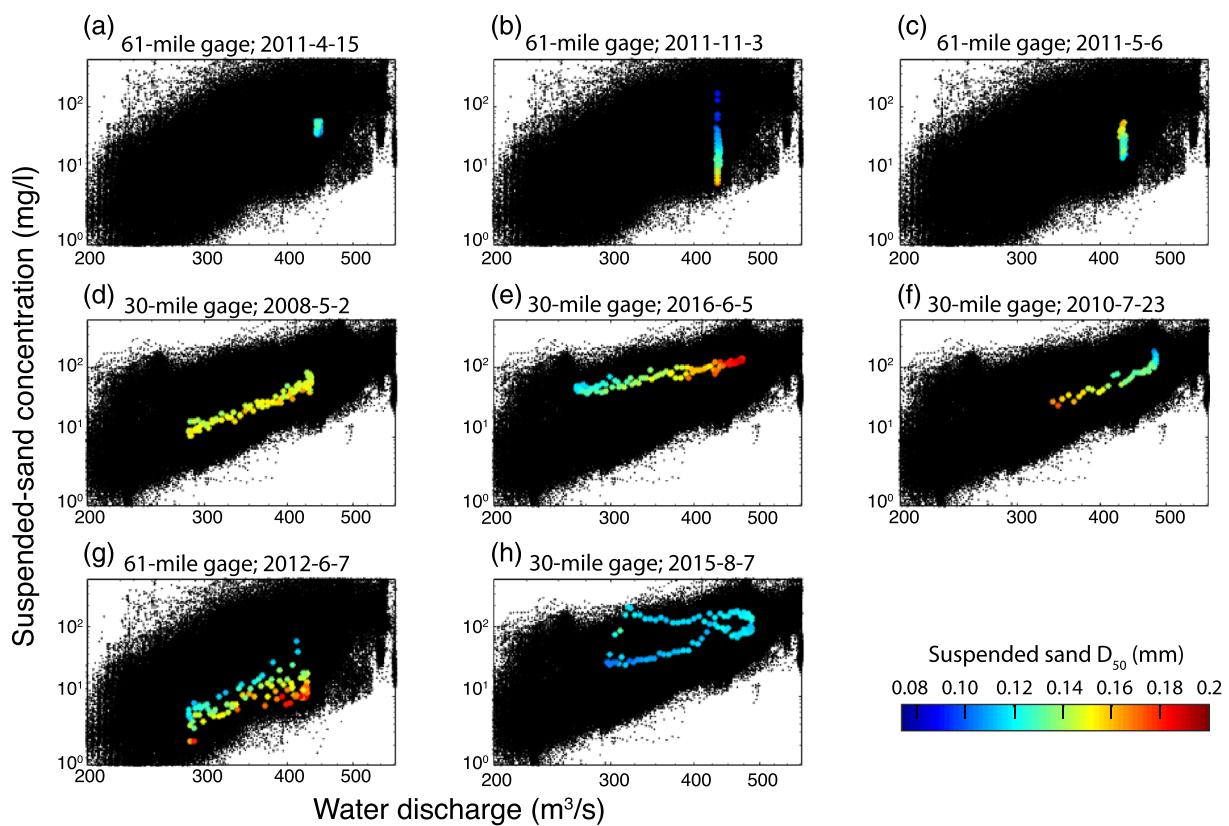


**Figure 7.** Concentration and grain size of suspended sand (large color-coded points) plotted as a function of water discharge for eight individual days selected from the 30- and 61-mile gages. Animations of the complete sets of daily rating curves at three gages are included in the supporting information. Small black points show all samples for the specified gage. Errors in concentration do not exceed a few tens of percent and therefore would not extend much beyond the colored points. Greater random error, if present, would obscure the clear patterns that are evident in some subplots. The top row shows 3 days at the 61-mile gage when discharge remained steady ( $\pm 5\%$ ), which occurred on only 599 days of the 4,281 days with at least 20 data points. (a) Concentration is nearly constant. This was an uncommon pattern even on days with steady flow; concentration varied by less than a factor of 2 on only 166 of the 599 steady-flow days. (b) Concentration and grain size are inversely correlated. This is the most common pattern for days with steady flow (474 of the 599 steady-flow days); it is the expected relation where concentration and grain size of suspended sand are regulated by grain size on the bed. (c) Concentration and grain size are positively correlated (125 of 599 steady-flow days). This is the dominant pattern at the 61-mile gage for the spring and early summer of 2011, when flows were unusually high. A positive correlation between suspended-sand grain size and concentration is expected where suspension is regulated by changes in flow (Rubin & Topping, 2001), but not on a day such as this, when discharge is constant. In the second row (d–f), measurements from the 30-mile gage show concentration increases with discharge, while grain size in suspension shows 3 different trends. In (d), grain size remains nearly constant; in (e), grain size increases with discharge; and in (f) grain size varies inversely with discharge. The bottom row (g and h) shows days at the 61- and 30-mile gages when concentration and discharge are more scattered. (g) Concentration increases with discharge and inversely with grain size. (h) Hysteresis loop with grain size varying only slightly.

during spring and summer 2011, when flows were both steady and unusually high. At these times and this location, the pattern was reversed, and concentration and grain size of suspended sand were positively correlated (Figure 7c). This positive correlation conflicts with Equation 4, indicating that concentration and grain size in suspension were influenced by other processes.

Reservoir releases typically fluctuate from day to night in response to regional electrical demand, and these daily fluctuations were used to examine how suspended sand responded to changes in flow. The second row in Figure 7 shows three such days with variable discharge at the 30-mile gage. On all 3 days concentration was positively correlated with discharge and showed little to no difference between rising and falling discharges. This was the dominant pattern for the 4,281 days on which discharge varied by more than  $\pm 5\%$ . The difference between the three cases is how  $D_s$  was related to  $C$  (and to discharge): no correlation (Figure 7d), positive correlation (Figure 7e), and inverse correlation (Figure 7f).

On most days with changing water discharge,  $C$  and  $D_s$  were inversely correlated at each discharge (Figure 7g), thus resembling the multiyear pattern in Figure 5. This pattern is consistent with Equations 1 and 2, if  $D_b$  had fluctuated up and down repeatedly while discharge underwent a single daily cycle. On a

few days with changing water discharge,  $C$  and  $D_s$  at each discharge were positively correlated. In the example in Figure 7h (30-mile gage), the daily observations display a hysteresis loop with little scatter. In this case, the conditions that caused  $C$  to vary at constant discharge changed slowly during the day, completing a single cycle.

A very small percentage of days with high concentrations of silt and clay exhibit a variety of patterns not shown in Figure 7, including days with higher concentrations of coarser sand in suspension. We do not know if these patterns are real or are merely artifacts of the acoustical algorithm that corrects for the large amount of backscatter from high silt and clay concentrations when computing suspended-sand concentration and median grain size (Topping & Wright, 2016). These data were excluded from the analysis, but we cannot rule out the possibility that tributary inputs or other processes caused short bursts having high concentrations of coarse sand. Although these measurements were not included in the statistical analysis, they are included in the individual movie frames in the animations (supporting information), with the silt and clay concentrations noted.

### 3.3. Relations Between Bed Sand and Suspended Sand

To further investigate the hypothesis that suspended sand is regulated by bed-sand grain size, we also evaluate whether the magnitude and timing of changes in grain size of sand on the bed  $D_b$  are sufficient to cause the observed changes in concentration  $C$ . According to Equation 5, if  $D_b$  changes by a factor of  $\Delta D_b$ ,  $C$  will change by  $\Delta D_b^K$  (at constant  $u_*$ ). Comparison of the lower and upper bounds of the curves in Figure 2 shows that mean bed-sand grain size varies by a factor of approximately 2.5, and Equation 5 thus predicts  $C$  to vary by  $2.5^K$ . Depending on the value of  $K$  (within the range of  $-3$  to  $-1.5$  determined by Rubin & Topping, 2001),  $C$  is predicted to vary by a factor of 4 to 16. Although this predicted range is substantial, it is nevertheless much smaller than the observed 2–3 order-of-magnitude variability in  $C$  for a given discharge shown in Figures 5 and 6. The large envelope in concentration, however, is due in part to the large number of observations of suspended sand at any given discharge.

A better approach to analyzing these changes is also based on Equation 5 but takes into account that the observed range in  $C$  arises from hundreds or thousands of measurements at any discharge, whereas the range in  $D_b$  (Figure 3) results from no more than 10 values (each of which is the mean grain size for one survey of a 20-km river segment). So, instead of comparing the unequally sampled ranges of the two respective measurements, we test Equations 1 and 5 by comparing the observed standard deviation of  $\log D_b^K$  with the standard deviation of  $\log C$ .

For the normalized measurements at the four gages (Figure 6 is one example), the mean standard deviation of  $\log C$  is 0.6. For the river segments in Figure 4,  $\log(D_b^K)$  varies through time with a mean standard deviation of 0.43 to 0.86 (depending on the value of  $K$ ). The observed temporal variability in  $D_b$  is thus sufficient to produce the observed temporal variability in suspended-sand concentration. The larger apparent range in concentration for any one discharge in Figure 5 arises in part because of the much larger number of data points that spread farther from the mean.

To demonstrate that Equation 5 accurately predicts  $C$ , not only must  $D_b$  and  $C$  vary by the appropriate amounts (as shown above) but the timing must also be in sync. This can be evaluated by calculating the covariance between the right and left sides of the equation. The term in brackets on the right side is normalized bed-sand grain size (“ $\beta$ ” of Rubin & Topping, 2001), which is defined as an observed bed-sand grain size  $D_b$  divided by mean  $D_b$ .

The left side of Equation 5 is normalized concentration, which is defined as the observed concentration divided by the best fit concentration for the discharge at which concentration was measured. At the 30-mile gage, the best power law fit is  $C = e^{-13.52} \times Q^{2.89}$ , where  $Q$  is water discharge in  $\text{m}^3/\text{s}$ ; at 61-mile, the best fit concentration is  $e^{-19.58} \times Q^{3.86}$ . The ratio of observed concentration to best fit concentration is a dimensionless measure of how high or low each measured concentration is relative to the best fit concentration for that water discharge.

Two decisions are required to evaluate Equation 5. The first decision is which measurements of  $D_b$  upstream from a gage are included in the calculations. The calculations below use all bed samples in the reach extending 20 km upstream from a gage, and a second set of calculations uses only samples from eddies in the same

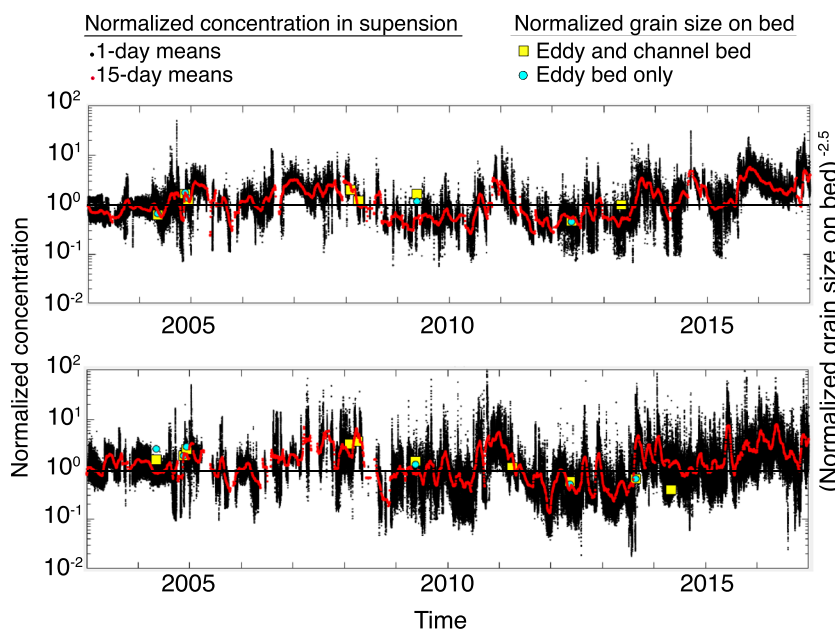


**Figure 8.** Plot of time series of the left and right sides of Equation 5. The left side of the equation is normalized  $C$  (observed concentration divided by the mean concentration for the discharge at which  $C$  was measured) and is shown by the black points (1-day means) and red points (15-day means). Normalization effectively removes  $u_*$  from the equation by calculating how high or low the concentrations are for the observed water discharge. The right side of Equation 5 is normalized bed-sand grain size  $D_b$  raised to an exponent of  $K$  and is shown by the yellow squares (channel and eddy bed sand) and blue dots (eddies only). Normalized  $D_b$  is defined as the mean size of sand observed on the bed divided by the mean grain size for all surveys of the same region of bed. In this case, the survey region extends 20-km upstream from the gage and includes samples where the bed is 0 to  $-24$  m below reference stage. Normalized grain size is defined as  $\beta$  (Rubin & Topping, 2001). Both plots use  $K = -2.5$ , which is the mean value observed. The median number of grain-size measurements used to calculate each bed-sand point is greater than 300, so the standard error of the mean is typically smaller than the size of each point plotted. Other than the value of  $K$  and choosing the size of spatial and temporal bins for averaging, no adjustable parameters were used to prepare the plot.

river segment. The second decision is what time window to use to average the normalized concentrations (to reduce the daily discharge-dependent variability). The calculations below use a 15-day window, although results are similar using a 10- or 20-day window. Despite the large number of observations of  $C$  and  $D_b$ , their time series have few measurements made at approximately the same time and location (from 3 to 10 pairs at the 30-mile gage, 61-mile gage, and Grand Canyon gage). This small number of paired measurements arises because bed sand was measured at few times, whereas suspended sand was measured at few locations.

To evaluate the performance of Equation 5, normalized bed-sand grain size and normalized concentration are used to solve for  $K$  at the 30-mile, 61-mile, and Grand Canyon gages. The calculated values are  $-3.0$ ,  $-2.8$ , and  $-2.4$ , respectively, which are in the more negative part of the range of  $-3.0$  to  $-1.5$  predicted by Rubin and Topping (2001). The squared correlations between the two sides of Equation 5 are low, ranging from 0.25 to 0.38. Results using  $D_b$  measurements restricted to the eddies are slightly different. Measurements of  $D_b$  in eddies are not available in the 20 km upstream from the Grand Canyon gage, so calculations are limited to the 30- and 61-mile gages. At these two gages,  $K$  is  $-2.1$  and  $-2.0$  (also within the predicted range), and the squared correlations are 0.53 and 0.09. The results for Equation 5 are qualitatively similar to results for Equation 4: values of the exponents are within the predicted range, but squared correlations are low.

To illustrate graphically the covariance between the two sides of Equation 5, they are both plotted in Figure 8. Because both sides of the equation are dimensionless, they can be plotted on the same dimensionless scale.  $K$  was set to  $-2.5$ , the mean of the five values listed above. If Equation 5 performed perfectly, then the points representing normalized bed-sand raised to an exponent of  $-2.5$  (right side of Equation 5) should plot directly on top of the time series of normalized  $C$  (left side of Equation 5). This is approximately true for some points, but other points deviate substantially, causing the low squared correlations.

## 4. Discussion

Previous studies have proposed a variety of causes of variability in  $C$ —some are listed in section 1.1—but direct comparison with those causes is difficult because many of them are, in fact, broad categories that encompass multiple physical changes in a channel. For example, sand supply, scour, or fill, the amount of sediment stored in a reach, and seasonal variability all have been proposed as causes of discharge-independent variability in  $C$ , but each of these causes can include multiple factors such as changes in grain size of sand on the bed (dependent on supply of different grain sizes), areal coverage of sand on the bed (dependent on total amount of sand and how it is distributed in a reach), topographic changes in the channel (dependent on sand supply and scour and fill), or changes in the boundary shear stress (where topographic change is sufficient to alter the flow).

This work focuses on two narrower questions: How much variability in  $C$  is caused by changes in  $D_b$ , and what processes cause the variability that is not explained by  $D_b$ ? These questions are addressed first in section 4.2, which reviews the extent to which results are consistent with variability in  $C$  being controlled by  $D_b$ . This is evaluated by how well the measurements conform to Equations 4 and 5. Next, section 4.3 considers what processes might cause variability in  $C$  that is not accounted for by  $D_s$  in Equation 4 or by  $D_b$  in Equation 5. This is done by considering what other processes operate with an appropriate magnitude, sign, and temporal and spatial scales. Although the specific processes that are most important in causing variability in  $C$  may differ from one river to another, the approach illustrated here can be applied to any river in which  $C$  varies at constant discharge.

### 4.1. How Bed-Sand Results Relate to Previous Work

#### 4.1.1. Longitudinal and Temporal Variability

Previous work (Topping, Rubin, Nelson, et al., 2000) found that fine sand introduced by large floods on Paria River in the 1990s could pass through Marble Canyon within days to weeks. The fine sand was detected as a secondary mode in the grain-size distribution of sand on the bed. Within 8 months after tributary inputs, bed sand became nearly as coarse as it was before the tributary floods (Topping, Rubin, Nelson, et al., 2000). Although the bed-sand surveys reported here show fining and coarsening through time (Figures 2–4), the longitudinal surveys did not detect pulses of fine tributary sand advancing downstream onto a bed of coarser sand. The surveys were evidently too infrequent, too long after tributary floods that supplied large amounts of sand, or too insensitive to tails of the grain-size distribution to detect such pulses before they were transported long distances downstream or mixed with sand already on the bed.

Although grain size of sand on the bed varies little among reaches at the times of our surveys, variability is substantial from one survey to another at any given location (Figures 2–4). Bed-sand measurements show a seasonal tendency, with many of the coarser grain sizes observed in May, when tributary inputs had undergone many months of winnowing. As reported above, the observed temporal variability of bed-sand grain size  $D_b$  is sufficient to cause a substantial proportion of the observed variability in  $C$  at a given water discharge.

#### 4.1.2. Bed-Sand Grain Size as a Function of Depth and Setting

The observed coarser grain size of bed sand in deeper parts of the channel (Figure 3) is consistent with the classical fining-upward sequence in fluvial sands (Allen, 1970). The significance of this trend in Grand Canyon is not that sand fines toward the riverbank but that this pattern occurs in bedrock canyons as well as alluvial rivers. Previous work has described other similarities between rivers in the two settings (Rubin et al., 1990).

The observation that bed-sand grain size in lateral separation eddies is finer than in the main channel has been reported previously (Schmidt, 1990; Schmidt et al., 1993). These studies have documented weaker flows, finer sand, and sorting by grain size within eddies in both flume experiments and in the Colorado River.

### 4.2. Which Results Are Consistent or Inconsistent With Equations 4 and 5?

Results that are consistent with the equations are (1)  $K/M$  calculated using Equation 4 is within the predicted range for the entire record of measurements at three of the four gages, and it is within the predicted range for most of the subsets of measurements in Figures 6b and 6c, (2)  $C$  and  $D_s$  are inversely correlated on nearly all days observed (e.g., Figures 7b and 7d–7g), (3)  $K$  calculated using Equation 5 is within the predicted range at

the gages where sufficient measurements are available, and (4) concentrations at a given discharge are usually similar on the rising and falling limbs of daily hydrographs (as in Figures 7d–7f), which demonstrates that disequilibrium effects are not a substantial cause of variability for the daily measurements (that were not excluded because of high silt or clay concentrations).

Measurements that are apparently inconsistent with the equations are as follows: (1)  $K/M$  is steeper than the predicted range at the Grand Canyon gage, (2)  $K/M$  for two subsets of measurements is outside the predicted range (including one subset with a positive slope at the 61-mile gage), (3) subsets of measurements have slopes in the predicted range but are offset to higher or lower concentrations (Figure 6b), (4) the mean squared correlation between  $\log C$  and  $\log D_s$  for the four gages is only 0.4, (5)  $C$  and  $D_s$  are positively correlated on some days (Figure 7c), and (6) Equation 5 accounts for less than half of the covariance between normalized bed-sand grain size and normalized concentration.

Nearly all of the variability in  $C$  that is not explained by Equation 4 is caused by physical processes in the river rather than measurement error. Residuals to Equation 4 are a factor of 14 for 95% of the measurements, whereas errors in measurements of  $C$  and  $D_s$  are only tens of percent (Table 1). To summarize the results, the observed relations between  $C$  and  $D_s$  (Equation 4) and between  $C$  and  $D_b$  (Equation 5) suggest that approximately half the variability in  $C$  and much of the range in  $C$  can be attributed to changes in grain size of sand on the bed.

#### 4.3. Processes Causing Variability Not Accounted for by Equations 4 and 5

##### 4.3.1. Changes in Standard Deviation of Bed-Sand Grain Size

When tributaries deliver fine sand to the Colorado River, not only does the mean bed-grain size become finer but also the new finer sand supply mixes with coarser sand already on the bed to produce a more poorly sorted grain-size distribution (Topping, Rubin, Nelson, et al., 2000). The broader distribution includes more sand in finer sizes than is accounted for by the mean size. This process occurred in 1983, when a factor of 2 decrease in  $D_b$  was accompanied by a factor of ~30 increase in predicted sand concentration (Topping et al., 2007). Topping et al. (2018) describe examples from other rivers where grain size of sand in suspension tracks better with the fine tail of the bed-sand grain-size distribution than with  $D_b$ .

The simplified approximations to Rouse's theory in Equations 1, 2, and 5 use an average  $D_b$  instead of the full grain-size distribution. Although  $K$  varies for different standard deviations of sand on the bed (Rubin & Topping, 2001, 2008), the equations do not account for the effects of changes in tails of the grain-size distribution unless the full grain-size distribution on the bed is measured, and  $K$  is specified to vary accordingly.

##### 4.3.2. Changes in $u_*$ at Constant Discharge

A likely cause of variability not described by the equations is that the water discharge through a cross section does not uniquely quantify the local boundary shear stress on the sandy areas of the bed. A common situation that causes shear stress to change is where deposition changes the local topography, thereby altering the local flow field. Topographic change can involve scour or fill (Colby, 1956; Topping, Rubin, Nelson, et al., 2000) or changes in the size and/or shape of lateral separation eddies (Schmidt, 1990). For example, a flood on the Paria River delivered so much sand to the Colorado River that the flow shallowed substantially, and sand antidunes formed at a site where the bed was normally gravel. Similarly, the 1996 experimental flood deposited as much as 5 m of sand within the 122-mile eddy. When the flow returned to its pre-flood discharge, the eddy became smaller, and the areas of the flood-deposited sand that were no longer within the eddy were subjected to strong downstream flow. Within a few days, a 3-m-high cut bank was scoured into the downstream end of the eddy bar (Rubin et al., 1998). As the bar eroded and supplied sand to the flow, transport rates at this point must have been much higher than before the bar was deposited (at the same discharge). Such changes in shear stress caused by changing topography are very common in Grand Canyon, and this process is also a likely cause of variability in concentration of suspended sand in alluvial rivers.

In the two examples cited above, changes in topography caused boundary shear stress to change, but shear stress over sandy regions in a segment of river can also change without substantial change in topography. For example, where sand is initially redistributed over gravel in a high-stress region of the bed (as in the first example described above), sand will be subjected to greater than usual stress without the topography changing substantially.

Development of dunes or other bedforms can affect  $u_*$  even when flow is constant. For example, coarsening of the bed during the steady flow of the 1996 flood experiment caused a rippled bed to change into dunes (Rubin et al., 1998), and development of the dunes can affect  $u_*$  (Smith & McLean, 1977). The dune measurements reported by Leary and Buscombe, (2020, Figure 2) demonstrate that bedforms respond almost instantly to changes in flow and that bedforms can double or even triple in size over relatively moderate changes in discharge. Changes in bedforms are not addressed by the equations in section 1.4, unless  $K$  and  $M$  are specified to change.

Previous field measurements and laboratory experiments have shown that lateral separation eddies pulsate even when flow is regulated to be constant (Rubin & McDonald, 1995). Such pulsations are commonplace and must cause  $u_*$  to vary, but their effect on sand transport has not been studied.

#### 4.3.3. Changes in Areal Coverage of Sand on the Bed

Areal coverage of sand on the bed in Grand Canyon has been observed to increase by a factor of 2 as sand was redistributed during controlled floods (Anima et al., 1998; Schmidt et al., 2007), and lab experiments and theory have shown that changes in areal coverage of sand on the bed influence suspended-sand concentration (Grams & Wilcock, 2007). Changes in areal coverage of sand of more than an order of magnitude were observed by Topping, Rubin, Nelson, et al. (2000) in association with the conversion of a deep gravel-bedded channel to a shallow sandy channel described in the previous section. Topping et al. (2007) attempted to quantify the importance of areal coverage of sand and found that changing the modeled area of sand by a factor of 2.5 was sufficient to bring modeled sand concentrations into agreement with observations. However, there were no independent observations of areal coverage with which to test the model results. Topping et al. (2007) also showed that changes in bed-sand grain size are sufficient to offset potentially opposing changes in bed-sand area in regulating suspended-sand concentration because the non-linear control of bed-sand grain size is strong enough to completely offset the approximately linear control (Grams & Wilcock, 2007) of bed-sand area on suspended-sand concentration. If changes in areal coverage are coupled to changes in  $u_*$ , however, the combined effect can have a greater impact on  $C$ , as described above.

#### 4.3.4. Variability of Grain Size as Function of River Stage

On some days, such as the day illustrated in Figure 7f,  $D_s$  is inversely correlated with discharge. This is opposite to lab experiments (Einstein & Chien, 1953; Guy et al., 1966), in which  $C$  and  $D_s$  are positively correlated when discharge changes (Rubin & Topping, 2001). The key difference between the two situations is that all grains on the bed were submerged at all discharges in the lab. In contrast, higher discharges on the Colorado River cause the river to inundate and potentially mobilize finer grains that, on average, are stored at higher elevations on sandbars (Figure 3). This process may explain why grain size in suspension is inversely correlated with discharge on some days.

Grain size of sand in the subsurface also varies with elevation (Rubin et al., 1990) and may influence  $D_s$  when the overlying sediment is removed by erosion. Until those deposits are exposed and available to the flow, however, they do not affect sand in suspension.

#### 4.3.5. Variability Not Accounted for by Eq 5

It might be expected that Equation 5 would perform better (higher squared correlations) than Equation 4 because Equation 5 relates concentration directly to the independent variable  $D_b$ , whereas Equation 4 relates concentration to  $D_s$  (another dependent variable). In fact, Equation 4 outperforms Equation 5. As noted by Rubin and Topping (2001), using  $D_s$  rather than  $D_b$  has several advantages. First, all measurements of  $D_b$  are counted equally when calculating average grain size. Not all areas of the bed have an equal influence on suspended sand, however, because different areas of the bed are subject to different values of  $u_*$ . In contrast,  $D_s$  is a representative sample of how the flow interacts with grains on the bed, giving greater weight to those areas of the bed that supply more sand to the flow. Sampling of grains by the flow may also include grains within the mobile layer (Dorrell et al., 2013), which may not be equally represented on the bed surface. Second, our measurements of  $D_b$  represent a mean size and therefore are not strongly influenced by the tails of the sediment size distribution. Although  $D_s$  also represents a mean value,  $D_s$  has disproportionately sampled the fine tails of the bed sand, and in this regard,  $D_s$  is more directly related to  $C$ .

Topping et al. (2005, 2008) concluded that grain size of sand in eddies is the dominant control of suspended sand in the river over multidecadal time scales. In the present study, results were inconsistent. The squared

correlations between the terms on the left and right sides of Equation 5 were calculated using eddy-only bed-sand measurements at two gages and using all bed-sand measurements at three gages. The two eddy-only correlations were the highest and lowest of the five measurements. It is plausible that these differences depend on whether eddies are acting as sources or sinks for sand at the time of the suspended-sand measurements, how many eddies are upstream from a gage, and how close individual eddies are to a gage, or other local topographic factors.

#### 4.3.6. Specific Deviations From Equation 4

The value of  $K/M$  at the Grand Canyon ( $-5.8$ ) is substantially more negative than the predicted range. Equation 4 assumes that  $u_*$  remains constant, but Equations 1 and 2 can be used to predict how a more negative  $K/M$  might arise where that condition is not met. For example, during times with little supply of sand from tributaries, scour and winnowing of sandy patches on the bed might cause  $D_b$  to increase (by disproportionately removing the finer grains from the sandy patches) and simultaneously cause  $u_*$  on the sandy regions of the bed to decrease (by preferentially excavating sand from locations where  $u_*$  was highest). To cause  $K/M$  to change from the central value of the theoretically predicted range ( $-3.8$ ) to the value observed at the Grand Canyon gage ( $-5.8$ ) would require that a change in  $D_b$  be accompanied by a change in  $u_*$  of approximately 15% of that amount. In other words, a coarsening of the bed by 100% accompanied by a 15% decrease in  $u_*$  is sufficient to cause  $K/M$  to change from  $-3.8$  to  $-5.8$ . Testing this hypothesis would require sequential maps showing spatial distribution of  $u_*$ , but we have no such observations.

Coarsening of the mean size of bed sand could similarly be expected to be coupled to reduction of the fine tail of the grain-size distribution or reduction of the areal coverage of bed sand. Although any of these coupled changes could cause steeper  $K/M$ , we do not know why they might be more important at the Grand Canyon gage than at the other three gages.

As described above, measurements from some time periods have similar slopes but are offset from the best fit power law. For example, the two subsets on the right side of Figure 6b have similar slopes but are offset by a factor of  $\sim 5$ . This indicates that the proportionality in Equation 4 has different values for the two subsets, with differences that persisted for 1–2 years in each subset. These observations support the hypothesis that small day-to-day changes in grain size cause  $C$  and  $D_s$  within a subset to vary as predicted by Equation 4 but that large changes (such as changes in topography or scouring by high flows) can cause substantial multiyear changes that are not addressed by Equation 4.

The timing of some flow changes supports this hypothesis. In particular, the two subsets of points that have slopes outside the predicted range occurred in April–August and September–October 2011. Discharges in the first of these two periods were abnormally high, and these flows likely scoured the bed, depleted sand, and altered the topography. This reasoning is consistent with previous work that found that predam Marble Canyon lost and accumulated sand finer than 0.25 mm seasonally (Topping, Rubin, & Vierra, 2000). The observation that similar patterns were observed at different gages more than 300 km apart during the same time periods suggests that the divergences from Equation 4 were caused by systematic changes in the river rather than local processes.

In some regards, the multiyear changes in Figure 6b resemble what happened in the Mississippi River during the 1993 flood. That flood caused changes in suspended sediment concentrations that persisted for 3 years (Horowitz, 2003). The cause in that case was inferred to be loss of sediment, although the specific physical factors (coarsening of sediment, reduction of areas with erodible sediment, or other changes) were not specified.

We are still puzzled by what processes caused the persistent positive correlations between  $C$  and  $D_s$  in April through October of 2011. The positive correlations occurred on individual days (Figure 7c) and for periods of months (Figure 6b). Most of the processes listed above operate too slowly to cause subdaily changes, and many cause negative correlation or no correlation between  $C$  and  $D_s$ . One exception is the development or migration of bedforms on the riverbed. Dunes of a variety of scales are common in the Colorado River, and continuous rotating-sonar observations demonstrate that the dunes commonly migrate multiple wavelengths per day (Rubin & Carter, 2006). When the positive correlations were observed at the 61-mile gage in 2011, the Froude number was high and possibly greater than 1, so if bedforms were present, they were likely antidunes. Migration of bedforms past a gage—or breaking of antidunes—might cause changes in  $u_*$  which cause  $C$  and  $D_s$  to vary with a positive correlation (Equations 1 and 2) and appropriate (subdaily) time scale.

#### 4.4. Relevance to EWI and EDI Measurements

The results presented here do not necessarily apply to EWI and EDI measurements. Those measurements are made across the full channel, thereby averaging out much of the spatial variability in suspended-sand arising from the distribution of sand on the bed and local flow in the cross section (Topping et al., 2011). Changes in bed grain size may account for a larger proportion of the variation in suspended-sand concentration in a full cross section than they do in the small part ensonified by the acoustic-Doppler profilers. Nevertheless, the at-a-point measurements reflect physical changes within the cross section, and some of these changes persist for multiyear periods.

#### 4.5. Future Improvements

Predictions of suspended-sand concentration can likely be improved by models that use maps of areal coverage of sand, measurements of the full grain-size distribution throughout the sandy areas (instead of only the mean or median grain size), and maps of local boundary shear stresses to calculate sand transport point by point over the area of the bed that is covered by sand. These measurements would require considerably more fieldwork than is typically conducted in a river, although future technological advances might increase the feasibility of collecting such measurements.

### 5. Conclusions

The conclusions arising from this work center on three topics: utility of the analytical techniques for evaluating causes of variability in suspended-sand concentration, results for the Colorado River in Grand Canyon, and applicability to other rivers.

The following approaches are useful in evaluating the influence of bed-sand grain size  $D_b$  and other factors on concentration of suspended-sand  $C$ :

1. Examining whether concentration  $C$  and suspended-sand grain size  $D_s$  vary inversely, as predicted by Equation 4. If this is the case, then variability is likely to be influenced by changes in  $D_b$ .
2. Quantifying how well the measurements fit with Equation 4. Is  $C$  proportional to  $D_s^{K/M}$  (with  $K/M$  in the range of  $-5$  to  $-2$ )? If not, other processes are probably more important in causing variability in  $C$ .
3. Measuring  $R^2$  between  $\log C$  and  $\log D_s$  to determine how much of the variance in  $C$  can be attributed to  $D_s$  (and indirectly attributed to  $D_b$ ).
4. Identifying subsets of measurements collected during different time periods, in which the relationship between  $C$  and  $D_s$  deviates systematically from Equation 4 and therefore results from causes that are not addressed by that equation.
5. Detecting variability that is not explained by Equation 4, by normalizing measurements of  $C$  and  $D_s$  (as illustrated in Figure 6).
6. Inferring changes in  $D_b$  from changes in  $C$ , as described by Equation 5.
7. An equation that predicts  $C$  from  $D_b$  (Equation 5) might be expected to perform better than one that predicts  $C$  from  $D_s$  (Equation 4) because  $D_b$  is the important independent variable, whereas  $D_s$  is another dependent variable. In fact, Equation 4 performs better (measured by squared correlation between predicted and observed  $C$ ). Regardless of how many bed-sediment measurements are made, they do not take into account that different locations of the bed (with different local shear stresses) exchange sand with the flow in different proportions. In contrast,  $D_s$  provides a natural integration of the sand-transport processes, giving more weight to those areas of the bed that exchange more sand with the flow.
8. Characterizing the overall performance of the equations presented in section 1.4 will depend on perspective. Evaluated by the squared correlations between predictions and observations, the equations do not perform well; for the complete time series, they explain less than half the covariance between  $C$  and  $D_s$  (Equation 4) or between  $C$  and  $D_b$  (Equation 5). On the other hand, these simplified approximations of the underlying sand-transport physics account for a substantially greater proportion of variability during selected time periods (days to years), and they account for an order of magnitude of variability in  $C$  at a constant discharge. Moreover, the equations succeed at this, utilizing only a few commonly measured sediment properties and little or no adjustment of coefficients.

Applying these analytical techniques to the Colorado River demonstrates the following:

1. For a given water discharge, concentrations span a factor of 23 (for 95% of the measurements). Squared correlations between  $C$  and  $D_s$  (Equation 4) and between  $C$  and  $D_b$  (Equation 5) indicate that grain size accounts for less than half of the variance in local suspended-sand concentration.
2. The variability in  $C$  that is not explained by Equation 4 is 1 order of magnitude for 95% of the residuals. This variability is due to physical processes that the equation does not describe: changes in the fine tail of the grain-size distribution of sand on the bed; changes in areal coverage of sand on the bed; changes in shear stress to which sand on the bed is subjected (either because the flow changes where sand is located or because sand is redistributed into areas with different shear stress); and changes in bed forms in the channel.
3. Variability that is not explained by grain size occurs on time scales as short as hours and as long as years. For example, concentration varies by as much as a factor of ~5 at constant water discharge and constant  $D_s$  during different multiyear time periods.
4. For the surveys reported here, mean grain size of sand on the bed varies relatively little longitudinally, but it varies substantially through time in a given 20-km river segment (as much as a factor of 4 to 5 between the coarsest and finest surveys). On average, riverbed sand in the deepest parts of the channel is more than twice as coarse as on shallow parts of the bed, and sand on the channel bed is 25% coarser than sand on the bed in eddies.

Applicability to other rivers is as follows:

1. Identifying the causes of variability in suspended-sand concentration is a longstanding problem in sediment transport (often described as shifting or unstable sand rating curves). Although some of the processes described above are more pronounced in supply-limited rivers, other processes, such as changes in flow arising from topographic changes, can be expected in any river.
2. The causes of variability almost certainly differ from one river to another, but the analytical techniques illustrated here can be applied to any river; they will be most useful in rivers where the variability in  $C$  is large.
3. Our observations illustrate why it can be difficult to accurately predict sand transport. Not only can concentration vary by more than an order of magnitude at a constant discharge but concentration can also systematically vary in different ways during different periods. Using a relation observed during one time period to predict concentration in other periods may lead to substantial errors. Because it is impossible to know a priori how channel and bed conditions will evolve, continuous long-term measurements may be required to characterize the range of possible channel conditions and to monitor sediment mass balance (Topping et al., 2018).

## Data Availability Statement

The bed-sand data (Tusso et al., 2020) are available at <https://doi.org/10.5066/P92Y65R8>, and the suspended sediment data used in this study are posted online at ([https://www.gcmrc.gov/discharge\\_qw\\_sediment/stations/GCDAMP](https://www.gcmrc.gov/discharge_qw_sediment/stations/GCDAMP)). Hydrographs for the gages are available online (at <https://maps.waterdata.usgs.gov/mapper/index.html>).

## References

- Allen, J. R. L. (1970). Studies in fluvial sedimentation; a comparison of fining-upwards cyclothsems, with special reference to coarse-member composition and interpretation. *Journal of Sedimentary Research*, 40, 298–323.
- Anima, R. J., Marlow, M. S., Rubin, D. M., & Hogg, D. J. (1998). Comparison of sand distribution between April 1994 and June 1996 along six reaches of the Colorado River in Grand Canyon, Arizona. U.S. Geological Survey Open-File Report 98-141, 33p.
- Barnard, P. L., Rubin, D. M., Harney, J., & Mustain, N. (2007). Field test comparison of an autocorrelation technique for determining grain size using a digital 'beachball' camera versus traditional methods. *Sedimentary Geology*, 201(1-2), 180–195. <https://doi.org/10.1016/j.sedgeo.2007.05.016>
- Buscombe, D. (2013). Transferable wavelet method for grain-size distribution from images of sediment surfaces and thin sections, and other natural granular patterns. *Sedimentology*, 60(7), 1709–1732. <https://doi.org/10.1111/sed.12049>
- Buscombe, D., & Rubin, D. M. (2012). Advances in the simulation and automated measurement of well sorted granular material: 2. Direct measures of particle properties. *Journal of Geophysical Research*, 117, F02002. <https://doi.org/10.1029/2011JF001975>
- Buscombe, D., Rubin, D. M., & Warrick, J. A. (2010). Universal approximation of grain size from images of non-cohesive sediment. *Journal of Geophysical Research*, 115, F02015. <https://doi.org/10.1029/2009JF001477>
- Camenen, B., & Larson, M. (2008). A general formula for non cohesive sediment transport. *Journal of Coastal Research*, 24(3), 615–627. <https://doi.org/10.2112/06-0694.1>

## Acknowledgments

The authors thank Ted Melis for helping to develop and implement the data-collection program for this work. Hank Chezar and Gerry Hatcher contributed to design and fabrication of hardware used for grain-size analyses. Hank Chezar and USGS volunteers helped collect the bed-sand images. Parker Alwardt helped process the bed-sediment images. Jon Perkins and Jon Major provided helpful reviews. Funding for this work was provided by U.S. Bureau of Reclamation to the U.S. Geological Survey Grand Canyon Monitoring and Research Center and by the U.S. Geological Survey Pacific Coastal and Marine Science Center. Any use of trade, firm, or product names is for descriptive purposes only and does not imply endorsement by the U.S. Government.

- Chezar, H., & Rubin, D. M. (2004). Underwater microscope system, U.S. Patent and Trademark Office, Patent Number 6,680,795, January 20, 2004, 9 p.
- Colby, B. R. (1956). Relationship of sediment discharge to streamflow, U.S. Geological Survey Open File Report, Reston, Virginia.
- Davis, J. C. (1986). *Statistics and Data Analysis in Geology* (p. 646). New York: John Wiley.
- Dolan, R., Howard, A., & Gallenbeck, A. (1974). Man's impact on the Colorado River in the grand canyon. *American Scientist*, 62, 392–401.
- Dorrell, R. M., Hogg, A. J., & Pritchard, D. (2013). Polydisperse suspensions: Erosion, deposition, and flow capacity. *Journal of Geophysical Research: Earth Surface*, 118, 1939–1955. <https://doi.org/10.1002/jgrf.20129>
- Draut, A. E., & Rubin, D. M. (2013). Assessing grain-size correspondence between flow and deposits of controlled floods in the Colorado River, U.S.A. *Journal of Sedimentary Research*, 83(11), 962–973. <https://doi.org/10.2110/jsr.2013.79>
- Edwards, T. K., & Glysson, G. D. (1999). Field methods for measurement of fluvial sediment, Techniques of Water-Resources Investigations of the U.S. Geological Survey, Book 3, Chap. C2, 89p.
- Einstein, H. A. (1950). The bedload function for bedload transportation in open channel flows, Technical Bulletin No. 1026, U.S.D.A., Soil Conservation Service, 1–71.
- Einstein, H. A., & Chien, N. (1953). Transport of sediment mixtures with large ranges of grain size, Mo. *River Dist. Sediment Ser.*, Univ of Calif Berkeley 2, 72p.
- Engelund, F., & Hansen, E. (1967). *A monograph on sediment transport in alluvial streams* (2nd ed.p. 62). Copenhagen: Teknisk Forlag.
- Garcia, M. (Ed) (2008). *Sedimentation engineering: Processes, measurements, modeling, and practice*, Reston, Virginia: American Society of Civil Engineers. <https://doi.org/10.1061/9780784408148>
- Garcia, M., & Parker, G. (1991). Entrainment of bed sediment into suspension. *Journal of Hydraulic Engineering*, 117(4), 414–435. [https://doi.org/10.1061/\(ASCE\)0733-9429\(1991\)117:4\(414\)](https://doi.org/10.1061/(ASCE)0733-9429(1991)117:4(414))
- Grams, P. E., Buscombe, D., Topping, D. J., Kaplinski, M., & Hazel, J. E. Jr. (2018). How many measurements are required to construct an accurate sand budget in a large river? Insights from analyses of signal and noise. *Earth Surface Processes and Landforms*, 44(1), 160–178. <https://doi.org/10.1002/esp.4489>
- Grams, P. E., Schmidt, J. C., Wright, S. A., Topping, D. J., Melis, T. S., & Rubin, D. M. (2015). Building sandbars in the Grand Canyon. *Eos, Transactions American Geophysical Union*, 96, 12–16. <https://doi.org/10.1029/2015EO030349>
- Grams, P. E., & Wilcock, P. R. (2007). Entrainment of fine sediment into suspension over a coarse immobile bed in equilibrium transport. *Water Resources Research*, 43, W10420. <https://doi.org/10.1029/2006WR005129>
- Greimann, B. P., & Holly, F. M. Jr. (2001). Two-phase flow analysis of concentration profiles. *Journal of Hydraulic Engineering*, 127(9), 753–762. [https://doi.org/10.1061/\(ASCE\)0733-9429\(2001\)127:9\(753\)](https://doi.org/10.1061/(ASCE)0733-9429(2001)127:9(753))
- Griffiths, R. E., Topping, D. J., Andrews, T., Bennett, G. E., Sabol, T. A., & Melis, T. S. (2012). Design and maintenance of a network for collecting high-resolution suspended-sediment data at remote locations on rivers, with examples from the Colorado River, U.S. Geological Survey Techniques and Methods, 8-C2, 44 p., <http://pubs.usgs.gov/tm/tm8c2/>
- Guy, H. P., Simons, D. B., & Richardson, E. V. (1966). Summary of alluvial channel data from flume experiments, 1956–61, USGS professional paper, 462-I, 96 p.
- Hazel, J. E., Jr, Kaplinski, M., Parnell, R., Kohl, K., & Schmidt, J. C. (2008). Monitoring fine-grained sediment in the Colorado River ecosystem, Arizona—Control network and conventional survey techniques, USGS Open-File Report 2008:1276 15 p. <https://pubs.usgs.gov/of/2008/1276/of2008-1276.pdf>
- Hazel, J. E., Jr, Kaplinski, M., Parnell, R., Kohl, K., & Topping, D. J. (2006). Stage-discharge relations for the Colorado River in Glen, Marble, and Grand Canyons, Arizona, USGS Open-File Report 2006:1243 7 p. <http://pubs.usgs.gov/of/2006/1243>
- Horowitz, A. J. (2003). An evaluation of sediment rating curves for estimating suspended sediment concentrations for subsequent flux calculations. *Hydrological Processes*, 17(17), 3387–3409. <https://doi.org/10.1002/hyp.1299>
- Kaplinski, M., Hazel, J. E., Jr., Grams, P. E., Kohl, K., Buscombe, D., & Tusso, R. (2017). Channel mapping river miles 29–62 of the Colorado River in Grand Canyon National Park, Arizona, May 2009, USGS Open-File Report 2017–1030.
- Leary, K. P. C., & Buscombe, D. (2020). Estimating sand bed load in rivers by tracking dunes: A comparison of methods based on bed elevation time series. *Earth Surface Dynamics*, 8(1), 161–172. <https://doi.org/10.5194/esurf-8-161-2020>
- Magirl, C. F. N., Webb, R., & Griffiths, P. (2008). Modeling water-surface elevations and virtual shorelines for the Colorado River in Grand Canyon, Arizona, USGS Scientific Investigations Report 2008–5075, 32p.
- McLean, S. R. (1992). On the calculation of suspended load for noncohesive sediments. *Journal of Geophysical Research*, 97(C4), 5759–5770. <https://doi.org/10.1029/91JC02933>
- Moog, D. B., & Whiting, P. J. (1998). Annual hysteresis in bed load rating curves. *Water Resources Research*, 34(9), 2393–2399. <https://doi.org/10.1029/98WR01658>
- Rouse, H. (1937). Modern conceptions of the mechanics of turbulence, transactions of the American Society of Civil Engineers, 102, Paper No. 1965, 463–543.
- Rouse, H. (1938). *Experiments on the mechanics of sediment suspension*, Proceedings, 5th International Congress for Applied Mechanics, 55, 550–554. New York: John Wiley & Sons.
- Rouse, H. (1939). *An analysis of sediment transportation in the light of fluid turbulence*. Washington D.C: U.S. Department of Agriculture, Soil Conservation Service, SCS-TR 25.
- Rubin, D. M. (2004). A simple autocorrelation algorithm for determining grain size from digital images of sediment. *Journal of Sedimentary Research*, 74(1), 160–165. <https://doi.org/10.1306/052203740160>
- Rubin, D. M., & Carter, C. L. (2006). *Bedforms and cross-bedding in animation*, SEPM atlas series, no. 2 Tulsa, Oklahoma: SEPM Society for Sedimentary Geology, DVD.
- Rubin, D. M., Chezar, H., Harney, J. N., Topping, D. J., Melis, T. S., & Sherwood, C. R. (2007). Underwater microscope for measuring spatial and temporal changes in bed-sediment grain size, from particle size to sediment dynamics, eds Hartmann D, Flemming B.W. *Sedimentary Geology*, 202(3), 402–408. <https://doi.org/10.1016/j.sedgeo.2007.03.020>
- Rubin, D. M., & McDonald, R. R. (1995). Nonperiodic eddy pulsations. *Water Resources Research*, 31(6), 1595–1605. <https://doi.org/10.1029/95WR00472>
- Rubin, D. M., Nelson, J. M., & Topping, D. J. (1998). Relation of inversely graded deposits to suspended-sediment grain-size evolution during the 1996 flood experiment in Grand Canyon. *Geology*, 26(2), 99–102. [https://doi.org/10.1130/0091-7613\(1998\)026<0099:ROIGDT>2.3.CO;2](https://doi.org/10.1130/0091-7613(1998)026<0099:ROIGDT>2.3.CO;2)
- Rubin, D. M., Schmidt, J. C., & Moore, J. N. (1990). Origin, structure, and evolution of a reattachment bar, Colorado River, Grand Canyon, Arizona. *Journal of Sedimentary Research*, 60, 982–991.

- Rubin, D. M., & Topping, D. J. (2001). Quantifying the relative importance of flow regulation and grain-size regulation of suspended-sediment transport ( $\alpha$ ), and tracking changes in bed-sediment grain size ( $\beta$ ). *Water Resources Research*, 37(1), 133–146. <https://doi.org/10.1029/2000WR900250>
- Rubin, D. M., & Topping, D. J. (2008). Correction to “Quantifying the relative importance of flow regulation and grain-size regulation of suspended sediment transport  $\alpha$  and tracking changes in grain size of bed sediment  $\beta$ ”. *Water Resources Research*, 44, W09701. <https://doi.org/10.1029/2008WR006819>
- Schmidt, J. C. (1990). Recirculating flow and sedimentation in the Colorado River in Grand Canyon, Arizona. *Journal of Geology*, 98, 709–724.
- Schmidt, J. C., & Grams, P. E. (2011). Understanding physical processes of the Colorado River, effects of three high-flow experiments on the Colorado River ecosystem downstream from Glen Canyon Dam, Arizona. Ed Melis, T. S., USGS circular 1366:17–51 <http://pubs.usgs.gov/circ/1366/>
- Schmidt, J. C., & Rubin, D. M. (1995). Regulated streamflow, fine-grained deposits, and effective discharge in canyons with abundant debris fans. In J. E. Costa, et al. (Eds.), *Natural and anthropogenic influences in fluvial geomorphology*, *Geophysical Monograph Series* (Vol. 89, pp. 177–195). Washington, D.C.: American Geophysical Union. <https://doi.org/10.1029/GM089p0177>
- Schmidt, J. C., Rubin, D. M., & Ikeda, H. (1993). Flume simulation of recirculating flow and sedimentation. *Water Resources Research*, 29(8), 2925–2939. <https://doi.org/10.1029/93WR00770>
- Schmidt, J. C., Topping, D. J., Rubin, D. M., Hazel, J. E., Jr., Kaplinski, M., Wiele, S. M., & Goeking, S. A. (2007). Streamflow and sediment data collected to determine the effects of low summer steady flows and habitat maintenance flows in 2000 on the Colorado River between lees ferry and bright Angel Creek, Arizona, USGS Open-File Report 2007-1268, 79p.
- Smith, J. D., & McLean, S. R. (1977). Spatially averaged flow over a wavy surface. *Journal of Geophysical Research*, 82(12), 1735–1746. <https://doi.org/10.1029/JC082i012p01735>
- Topping, D. J., Mueller, E. R., Schmidt, J. D., Griffiths, R. E., Dean, D. J., & Grams, P. E. (2018). Long-term evolution of sand transport through a river network: Relative influences of a dam versus natural changes in grain size from sand waves. *Journal of Geophysical Research: Earth Surface*, 123, 1879–1909. <https://doi.org/10.1029/2017JF004534>
- Topping, D. J., Rubin, D. M., Grams, P. E., Griffiths, R. E., Sabol, T. A., Voichick, N., et al. (2010). Sediment transport during three controlled-flood experiments on the Colorado River downstream from Glen Canyon Dam, with implications for eddy-sandbar deposition in Grand Canyon National Park, USGS Open-File Report 2010-1128, 111p.
- Topping, D. J., Rubin, D. M., & Melis, T. S. (2007). Coupled changes in sand grain size and sand transport driven by changes in the upstream supply of sand in the Colorado River: Relative importance of changes in bed-sand grain size and bed-sand area. *Sedimentary Geology*, 202(3), 538–561. <https://doi.org/10.1016/j.sedgeo.2007.03.016>
- Topping, D. J., Rubin, D. M., Nelson, J. M., Kinzel, P. J. III, & Bennett, J. P. (1999). Linkage between grain-size evolution and sediment depletion during Colorado River floods. In R. H. Webb, J. C. Schmidt, G. R. Marzolf, & R. A. Valdez (Eds.), *The 1996 controlled flood in Grand Canyon*, *Geophysical Monograph* (Vol. 110, pp. 71–98). Washington, D.C.: American Geophysical Union.
- Topping, D. J., Rubin, D. M., Nelson, J. M., Kinzel, P. J. III, & Corson, I. C. (2000). Colorado River sediment transport 2. Systematic bed-elevation and grain-size effects of sand-supply limitation. *Water Resources Research*, 36, 543–570.
- Topping, D. J., Rubin, D. M., & Schmidt, J. C. (2005). Regulation of sand transport in the Colorado River by changes in the surface grain size of eddy sandbars over multi-year timescales. *Sedimentology*, 52(5), 1133–1153. <https://doi.org/10.1111/j.1365-3091.2005.00738.x>
- Topping, D. J., Rubin, D. M., & Schmidt, J. C. (2008). Update on regulation of sand transport in the Colorado River by changes in the surface grain size of eddy sandbars over multiyear timescales, USGS Scientific Investigations Report 2008-5042, 24 p.
- Topping, D. J., Rubin, D. M., Schmidt, J. C., Hazel, J. E., Melis, T. S., Wright, S. A., et al. (2006). Comparison of sediment-transport and bar-response results from the 1996 and 2004 controlled experiments on the Colorado River in Grand Canyon, CD Federal Interagency Sediment Conference, Reno, NV.
- Topping, D. J., Rubin, D. M., & Vierra, L. E. Jr. (2000). Colorado River sediment transport 1. Natural sediment supply limitation and the influence of Glen Canyon Dam. *Water Resources Research*, 36, 515–542.
- Topping, D. J., Rubin, D. M., Wright, S. A., & Melis T. S. (2011). Field evaluation of the error arising from inadequate time averaging in the standard use of depth-integrating suspended-sediment samplers, USGS Professional Paper 1774, 95p. <http://pubs.usgs.gov/pp/1774/>
- Topping, D. J., & Wright, S. A. (2016). Long-term continuous acoustical suspended-sediment measurements in rivers—Theory, application, bias, and error, USGS Professional Paper 1823, <https://doi.org/10.3133/pp1823>
- Tusso, R. B., Rubin, D. M., Buscombe, D., Hazel, J. E., Jr., Topping, D. J., & Grams, P. E. (2020) Measurements of bed grain size on the Colorado River in Grand Canyon National Park, Arizona: 2000 to 2014, Arizona: U.S. Geological Survey data release, <https://doi.org/10.5066/P92Y65R8>
- van Rijn, L. C. (1984). Sediment transport. Part II: Suspended load transport. *Journal of Hydraulic Engineering*, 110, 1613–1641.
- Vanoni, V. A. (Ed) (1975). *Sedimentation engineering, manual and reports on engineering practice 54*, New York: American Society of Civil Engineers.
- Walling, D. E. (1977). Assessing the accuracy of suspended sediment rating curves for a small basin. *Water Resources Research*, 13(3), 531–538. <https://doi.org/10.1029/WR013i003p00531>
- Warrick, J. A., Rubin, D. M., Ruggiero, P., Harney, J., Draut, A. E., & Buscombe, D. (2009). Cobble Cam: Grain-size measurements of sand to boulder from digital photographs and autocorrelation analyses. *Earth Surface Processes and Landforms*, 34(13), 1811–1821. <https://doi.org/10.1002/esp.1877>
- Wren, D. G., Bennett, S. J., Karkdolla, B. D., & Kuhnle, R. A. (2000). Studies in suspended sediment and turbulence in open channel flows, Research Report 18, U.S. Department of Agriculture, Research Report No. 18. National Sedimentation Laboratory, Oxford, Mississippi, USA.
- Wright, S., & Parker, G. (2004a). Density stratification effects in sand-bed rivers. *Journal of Hydraulic Engineering*, 130(8), 783–795. [https://doi.org/10.1061/\(ASCE\)0733-9429\(2004\)130:8\(783\)](https://doi.org/10.1061/(ASCE)0733-9429(2004)130:8(783))
- Wright, S., & Parker, G. (2004b). Flow resistance and suspended load in sand-bed rivers: Simplified stratification model. *Journal of Hydraulic Engineering*, 130(8), 796–805. [https://doi.org/10.1061/\(ASCE\)0733-9429\(2004\)130:8\(796\)](https://doi.org/10.1061/(ASCE)0733-9429(2004)130:8(796))
- Wright, S. A., Topping, D. T., Rubin, D. M., & Melis, T. S. (2010). An approach for modeling sediment budgets in supply-limited rivers. *Water Resources Research*, 46, W10538. <https://doi.org/10.1029/2009WR008600>